EXPLORING DIGITAL OSTEOLOGY COLLECTIONS WITH GEOMETRIC MORPHOMETRY TO CATEGORIZE FUNCTION AND PHYLOGENY

by
Travis Helm

A thesis submitted as partial fulfillment
of the requirements for the degree of

Masters of Science in
Geology

Idaho State University

August 2017

In presenting this thesis in partial fulfillment of the requirements for an advanced degree at Idaho State University, I agree that the Library shall make it freely available for inspection. I further state that permission for extensive copying of my thesis for scholarly purposes may be granted by the Dean of Graduate studies, Dean of my academic division, or by the University Librarian. It is understood that any copying or publication of this thesis for financial gain shall not be allowed without my permission.

Signature _____

Date _____

Committee Approval to the Graduate Faculty: The members of the committee appointed to examine the thesis of Travis Helm find it satisfactory and recommend that it be accepted.

_____

Leif Tapanila,
Major Advisor

_____

Paul Link,
Committee Member

_____

Curt Anderson,
Graduate Faculty Representative

Acknowledgments

First I would like to thank my advisor, Leif Tapanila, for his support, willingness to meet, help find funding, answer questions and provide many resources throughout my thesis. Second, I would like to thank my committee member Paul Link for taking interest in my project and guidance through his edits. Third, I would like to thank my graduate faculty representative Curt Anderson for not holding back with asking questions and helping me take a step back and learn how to explain my project in a way that the general public can understand.

I would also like to thank everyone in the Idaho Virtualization Lab for a great internship experience. I won't forget the many laughs we've shared and the random conversation topics that would come up out of nowhere. Anytime I had questions or needed some models for my project Bob, Nick and Jesse were there for me and supported me throughout my time in the lab.

Thank you to the friends I have made during this experience within the department and the sense of community the department provided. There was so much help and support I received when it came to questions I had and I appreciate everyone who took the time to help with whatever I needed.

Thank you to Mike and Kathy Luras who have opened up their home to me and made me feel like a member of their family.

A huge thank you goes out to my family who have supported me and encouraged me throughout this experience. Their support and encouragement gave me the motivation to pursue a master's degree.

Most importantly, I would like to thank my wife Lindsay and son Beckham for their unconditional love and support. There have been many highs and lows during this project and they have supported and encouraged me throughout. Thank you Beckham for always making me smile with his goofiness and personality. Thank you Lindsay for always being there to talk or listen when I needed you most. Both of their love and support they provided me helped me more than words can describe.

TABLE OF CONTENTS

List of Figures

List of Tables

ABSTRACT:

The field of morphometrics has produced a general understanding of shape variations among organisms. Three-dimensional data collection tools are more affordable, creating an increase in digital collections. These digital collections can be made available in multiple formats and the sharing of these data has increased through numerous and expanding digital collections.

Exploration of a digital osteology collection of mammals and birds using geometric morphometry is the goal of this study. In studying femur and humerus bones, it was determined that the most effective method for the geometric morphometric study was a 50-sliding landmark method. A principle component analysis demonstrates an expected result that bone shape correlates with both phylogeny and functional morphology. The categorization of phylogeny and simplifying the principle component analysis to meristic ratios allowed new "unknown" specimens to be evaluated in morphospace, including fossil taxa. These new elements plotted within the appropriate locomotion group field and near individuals of similar class, order and families. Results show a methodology for using digital osteology collections as a reference database.

1. INTRODUCTION:

The field of morphometrics has provided a general understanding of bone shape and variation among living organisms. Factors such as phylogeny, locomotion, body size, behavior and environment play key roles in variation of shape among organisms (Leach, 1961; Hildebrand, 1974; Miller et al., 1964; McGowan, 1999). Advancements in data collecting tools and increased accessibility of digital osteology collections make exploration of shape variations among organisms possible in a way not yet observed within the field of morphometrics. The goal of this study is to explore digital osteology collections using geometric morphometry to categorize phylogeny and function. The focus of this study is on the three-dimensional (3D) shape of forelimb and hindlimb long bones, consisting of multiple classes, orders, families and locomotor habits. Locomotor habits of the specimens of the study include arboreal, semiaquatic, aquatic cursorial for Mammalia and elliptical, high-lift, high-speed and dynamic soaring habits for Aves. A blueprint of bone shape for these specimens is outlined through literature review.

Arboreal animals have very spherical heads on the humerus and femur. The patellar surface of the femur is shallow and the capitulum of the humerus is broad to increase climbing ability and flexibility. Muscle attachments are decreased, therefore, decreasing strength in the animal. The decreased attachments however, allow for the bone to be lighter and the animal more agile. Hind limb bones are elongated, gracile and are most similar to cursorial proximal limb bones (Hildebrand, 1974; Hildebrand & Goslow, 2001; Samuels & Valkenburgh, 2008; Fabre et al., 2015; Fig. 1.1; Fig. 1.2).

The humeri for cursorial mammals have a head facing more proximal than other animals. Many of the major muscle attachments of the humerus are located at the

proximal end and there is a reduction of attachments for abductor and adductor muscles. Locomotion is therefore restricted to the line of motion of the animal. This restricted locomotion in the line of travel is also due to a larger trochlea, which creates a larger hinge structure (Hildebrand, 1974; McGowan, 1999; Polly, 2007; Fig. 1.1). The femora of cursorial mammals have large muscle attachments near the proximal end, resulting in a shorter and more robust bone. The greater trochanter is long and robust in cursors for muscle attachments of extensor and flexor muscles. The patellar surface at the distal end of the femur is longer and deeper in cursors (Hildebrand, 1974; McGowan, 1999; Polly, 2007; Fig. 1.2).

The major shape distinctions of semiaquatic mammals are short robust femora. They also have robust humeri that feature large muscle attachments making them beneficial for swimming (Samuels & Valkenburgh, 2008).

The humeri of aquatic mammals are robust with spherical heads, and have large distal articulations, lateral epicondyles and deltoid tuberosities. Larger muscle attachments on the humerus allow for larger stronger muscles that are used for extension, flexion, and rotation of the forelimb in swimming. The capitulum at the distal end of the humerus is more round allowing for increased rotation of the radial head (Hildebrand, 1974; Hildebrand & Goslow, 2001; Polly, 2007; Samuels & Valkenburgh, 2008; Fabre et al., 2015; Fig. 1.1). The femora of aquatic mammals in this study are short, robust and major changes include the lack of the fovea capitis on the femoral head and the reduction or loss of the lesser trochanter (Adam, 2009; Fig. 1.2).

The humeri of the birds in this study are relatively similar in shape. Major changes are seen between birds with high-speed and elliptical classified wings representing short and

robust wings, dynamic soaring birds representing elongated gracile wings, and high-lift birds representing elongated robust wings (Hildebrand, 1974; McGowan, 1999; Fig. 1.1). The femora of birds however are more distinct in shape. The femora of aquatic diving birds are short and stout. Muscle attachments are enlarged for extensor muscles, which are used as the primary powerstroke for diving (King & McLelland, 1985).

Perching birds have increased muscle attachments for muscles involved in femoral retraction. The neck and trochanter are more robust to absorb the stresses of landing (Hildebrand, 1974; King & McLelland, 1985; Fig. 1.2).

Extensive literature documents how humerus and femur shape variation is constrained among vertebrates. What has changed since the mid-2000's is the way morphological data is obtained and analyzed. The mid-2000's saw an increase in technology used for 3D data acquisition, however, access to 3D data acquisition tools was limited due to the high costs and complexity of the software (Kuzminsky & Gardiner, 2012). Within the last decade, access to high resolution and low cost 3D scanners and photogrammetry have become more readily available (Loy, 2007; Mitteroecker & Gunz, 2009; Loy & Slice, 2010). Increased access to this technology and a decrease in the cost and complexity of the software, has led to an increase in 3D digital osteology collections. These collections can be easily shared through multiple formats, benefiting the greatest audience (Elton & Cardini, 2008; Gippoliti et al., 2014; Cooke & Terhune, 2015). Researchers who are in isolated locations or lack necessary funding can access these digital collections while saving both time and money. Original collections are handled less, reducing the wear and tear and potential damages (Loy & Slice, 2010). The growth of these digital collections will continue to be facilitated with the continued

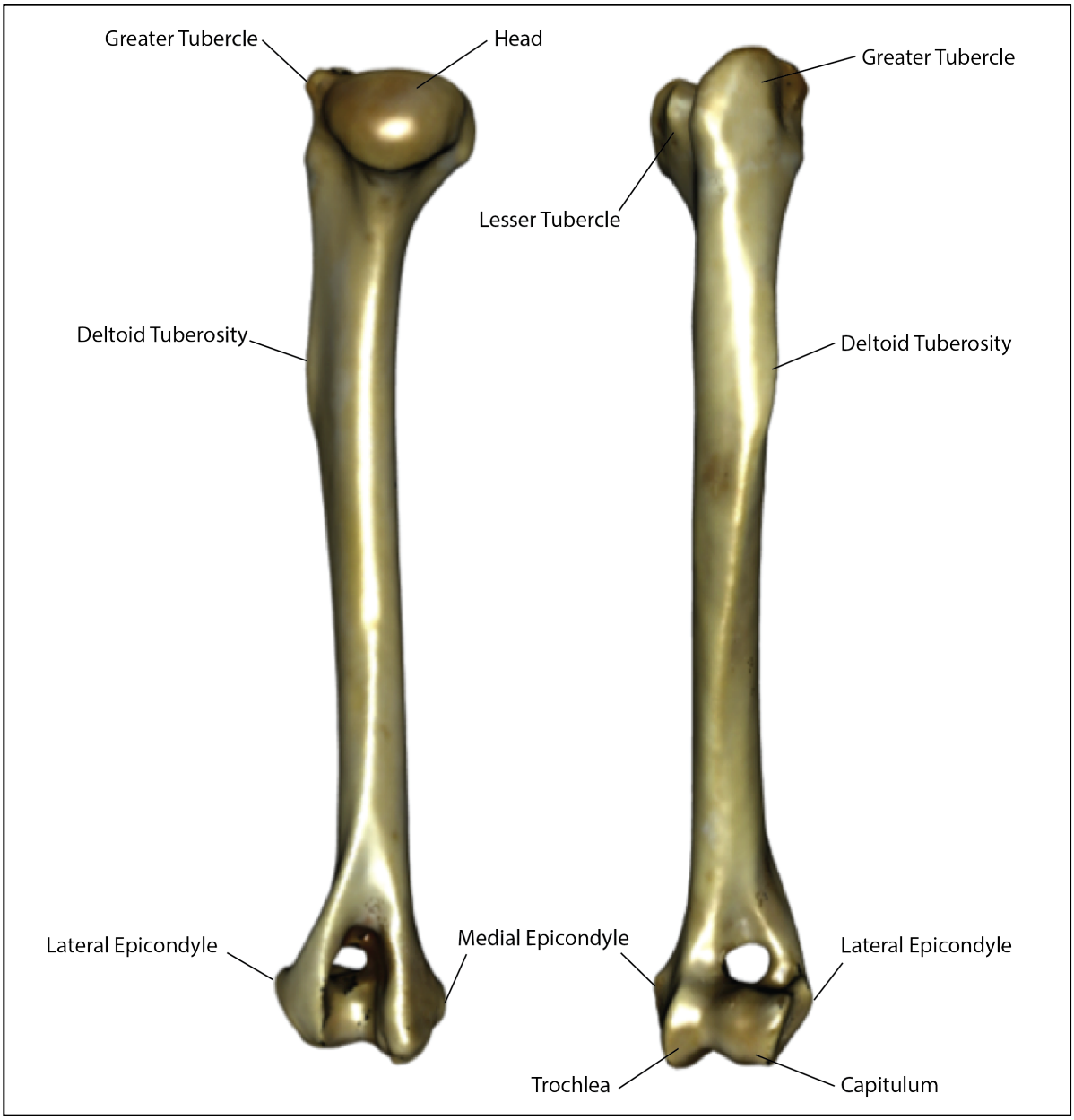

Fig. 1.1. Anatomy of the humerus bone

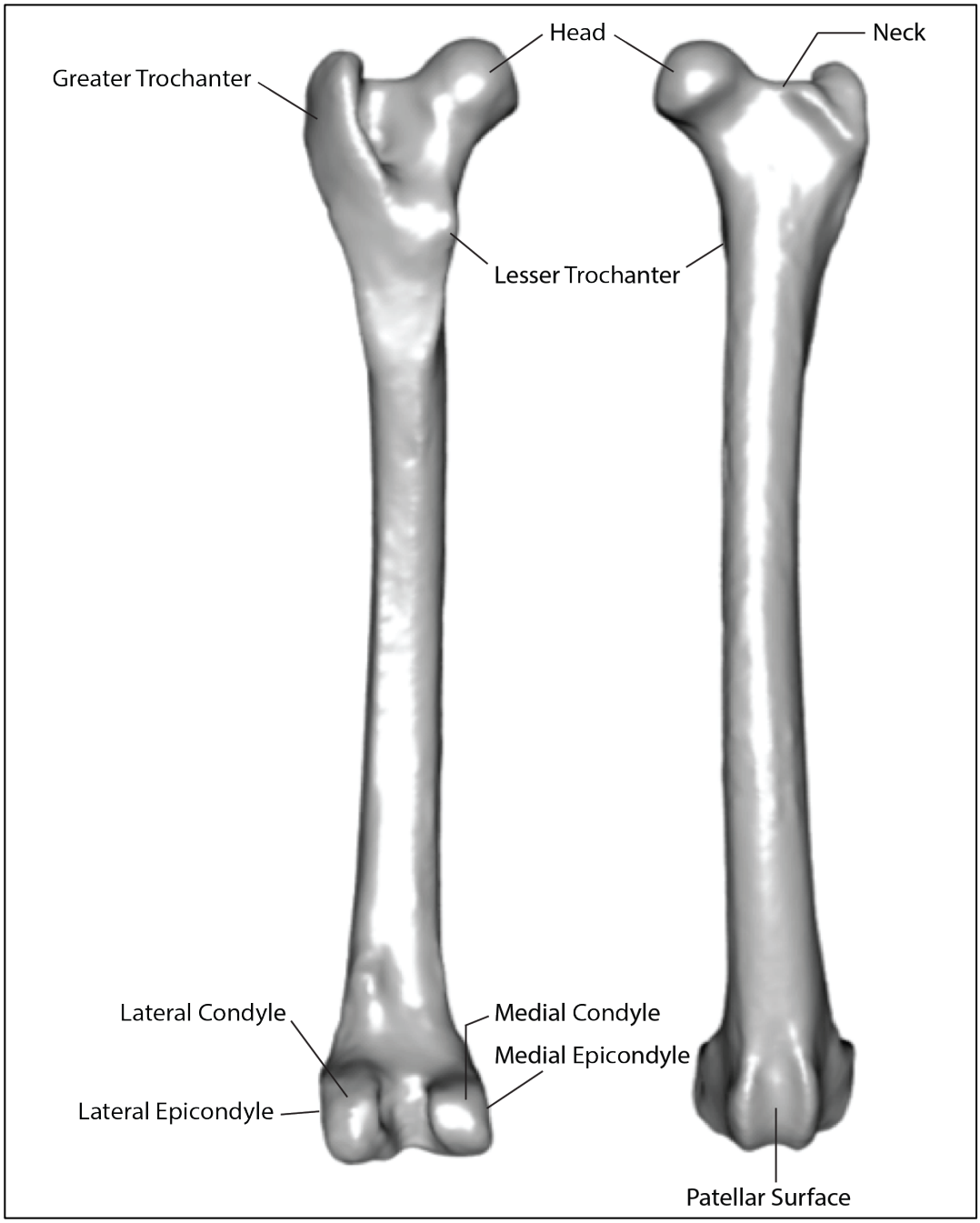

Fig. 1.2. Anatomy of femur bone

developments and reduced costs of data acquisition tools (Kuzminsky & Gardiner, 2012). An increase in these digital osteology collections gives researchers access to increased datasets that can be used in future morphometric studies.

Exploration of these diverse digital osteology collections with 3D geometric morphometry to categorize phylogeny and functionality is the goal of this study. Using 3D geometric morphometric methods, the non-shape variables of the bones in this study are eliminated leaving only bone shape to be analyzed and compared. The exploration of these collections led to the three main components of this study: (1) determine what landmark method and landmark quantity is most appropriate for the diverse dataset seen within this study; (2) categorize and recognize patterns of phylogeny and functionality; and (3) create a method to predict unknown specimens.

2. MATERIALS AND METHODS:

Materials

This study includes 62 left humeri and 74 left femora of arctic fauna consisting of 84 adult species (Appendix I). The humeri consist of individuals from of 62 species, 25 families, 12 orders and 2 classes (Appendix II). The femora consist of individuals from 74 species, 26 families, 14 orders and 2 classes (Appendix III). The specimens of this study were obtained through the NSF funded Virtual Zooarchaeology of the Arctic Project (VZAP), a digital collection created by collaboration with the Burke Museum of Science and Culture, Idaho Museum of Natural History, Smithsonian Institute, Museum of the North, and the Canadian Museum of Civilization. VZAP digitized faunal remains of species from northern latitudes to create an online digital collection. Archeologists and faunal analysts use the collection for comparative osteology as an aide for identification of remains during excavations (Maschner et al., 2011).

An additional 17 femora and 15 humeri of mammal and birds were used to test the categorization efficiency of the VZAP collection. These specimens were chosen because they represent species that are not within the original dataset, their locomotor groups are diverse and they consist of both extant and extinct species. These specimens were obtained through the VZAP and Idaho Museum of Natural History collections and all specimens are available through the Virtual Museum of Idaho at www.virtual.imnh.isu.edu.

Data Collection

The 3D digital models of the femur and humerus bones were acquired using either a Next Engine scanner, Cyberware M15 desktop scanner, or a Konica Vivid 9i laser

scanner (Maschner et al., 2011). The 3D models were uploaded into Mesh Lab and saved in the .ply format to make them compatible with Geomorph software. The entirety of this 3D sliding-landmark geometric morphometric study was completed in the Geomorph library in R (Adams & Otarola-Castillo, 2013; R Core Team, 2014).

Landmark Analysis

Results between fixed and sliding-landmark methods were compared to determine a landmark method that was most appropriate for this study. The quantity of landmarks placed for the sliding-landmark approach was also analyzed to compare results and determine how many landmarks are necessary for this study. The criteria used to determine the appropriate method include: (1) a good separation of specimens in principle component space; (2) maximization of PC1 variance as a percentage; and (3) reduction of total area among specific classifier groups.

The femora were used to compare landmark methods and landmark quantities. The fixed landmark approach used 7-fixed type-two landmarks (Table 2.1). The fixed landmarks are selected individually on the digitized bone model on homologous structures and in the same order for each specimen of the study (R Core Team, 2014).

A 3D sliding-landmark approach creates sliding semi-landmarks on the surface of the bones (Bookstein, 1996; Gunz et al., 2005; Fabre et al., 2015). Sliding semi-landmarks are landmarks that slide across the surface of a bone until they align in the most optimal way to points of a reference specimen (Adams et al., 2004). A landmark template was created for each quantity test of sliding landmarks. The sliding-landmark approach retains the 7-fixed type-two landmarks that act as sliding-landmark boundaries. An additional 50, 250, 500 and 1,500 sliding-landmarks were placed for the landmark

quantity comparisons. The sliding-landmarks of each additional femur of the study align to the template by sliding across the surface of the bone, creating geometrically semi-homologous landmarks (Adams et al., 2013; Adams & Otarola-Castillo, 2013; R Core Team, 2014). These sliding-landmarks can be treated as semi-homologous structures among the individuals because the method transforms the sliding-landmarks into geometric landmarks and the landmark data can be retained throughout the analysis (Rohlf, 2000; Slice, 2007; Holliday & Friedl, 2013; Gonzalez et al., 2016).

Comparisons of results for the landmark method analysis used visualization tools such as a principle component analysis, thin-plate spline deformation grids and vector displacements. Excel graphs were also used to compare landmark methods to eigenvalues for PC1, area of locomotor groups, group overlap and total overlap.

Landmark Placement

A 3D sliding-landmark approach was performed in the R package Geomorph on the femora and humeri of this study. The landmark placement for the femora consists of 7-fixed type-two and 50 sliding-landmarks, resulting in a total of 57 landmarks spread across each specimen (Table 2.1). Similar to the femora, the landmark placement for the humeri consists of 7-fixed type-two and 50 sliding-landmarks resulting in a total of 57 landmarks (Table 2.2).

General Procrustes Analysis

With landmark coordinates established, a general Procrustes analysis (GPA) transforms the data using the Geomorph library in R (Adams et al., 2013; Adams & Otarola-Castillo, 2013; R Core Team, 2014). The GPA eliminates non-shape variables such as location, orientation and scale by scaling, translating and superimposing all

Table 2.1. Definitions of landmark placement of the femora used in the study.

Landmark	Definition
1	Proximal apex of the greater trochanter
2	Distal apex of the neck
3	Proximal apex of the head
4	Lateral apex of the lateral condyle
5	Medial apex of the medial condyle
6	Anterior apex of the internal condyle
7	Anterior apex of the external condyle
Sliding-landmarks	Spread across bone to minimize bending energy

Table 2.2. Definitions of landmark placement of the humeri used in the study.

Landmark	Definition
1	Proximal apex of the greater tubercle in mammals and external tuberosity in Aves
2	Proximal apex of the head
3	Proximal apex of the lesser tubercle in mammals and internal tuberosity in Aves
4	Lateral apex of lateral epicondyle in mammals and ectepicondyle in Aves
5	Distal apex of trochlea in mammals and internal condyle in Aves
6	Distal apex of capitulum in mammals and external condyle in Aves
7	Medial apex of medial epicondyle in mammals and entepicondyle in Aves
Sliding-landmarks	Spread across bone to minimize bending energy

specimens within a common coordinate system (Loy, 2007; Cooke & Terhune, 2015). What remains is a mean shape without the influence of size, and the variation among the individual's landmark coordinates represents shape variation, which then can be analyzed (Slice, 2007; Adams et al., 2004; Galland & Friedl, 2016).

Principle Component Analysis

Visualization of shape variation and shape patterns are made possible through graphical methods such as a Principle Component Analysis (PCA). The PCA for this study was done using the Geomorph library in R (Adams & Otarola-Castillo, 2013; R Core Team, 2014). A PCA reduces a large set of variables to a few dimensions that represent most of the variation in the data (Mitteroecker & Gunz, 2009; Cooke & Terhune, 2015). Principle component (PC) scores assign values to each specimen along independent axes that maximize the shape variation within the group (Rohlf & Marcus, 1993; Adams et al., 2013).

Data classifiers categorize phylogeny and functionality within the morphospace of the PCA plots. The phylogenetic classifiers used in this study are class, order and family. The functional classifiers are based on locomotor habits for the individuals of the study as defined for the femora and humeri (Savile, 1957; Dial, 2003; Biancardi & Minetti, 2012; Fabre et al., 2013; Samuels et al., 2013; Dumont et al., 2016). Locomotion habits for the humeri include high-speed, high-lift, dynamic soaring, and elliptical for the Aves and cursorial, arboreal, semiaquatic and aquatic for Mammalia (Table 2.3). Locomotion habits for the femur include walk, perch, and swim/walk for the Aves and cursorial, arboreal, semiaquatic and aquatic for Mammalia (Table 2.4).

Table 2.3. Locomotor habits and definitions used in this study for the humerus analysis (from Savile, 1957; Dial, 2003; Fabre et al., 2013; Samuels et al., 2013).

Locomotion Habit	Definition
Cursorial	Species that have the ability to run fast or across large distances
Arboreal	Species that spend the majority of their time in trees to forage, escape and seek shelter
Semiaquatic	Species with the ability to live on land and in the water
Aquatic	Species that spend the most of their time in water
Elliptical	Birds that maneuver in shrub lands or forested habitats
High-speed	Birds that feed on the wing or make long migrations
High-lift	Birds that takeoff and land in fairly confined areas, exhibit high lift, low speed soaring, and slow descents
Dynamic soaring	Birds that glide over large expanses of water and have exploited the sea winds

Table 2.4. Locomotor habits and definitions used in this study for the femur analysis (from Savile, 1957; Dial, 2003; Fabre et al., 2013; Samuels et al., 2013).

Locomotion Habit	Definition
Cursorial	Species that have the ability to run fast or across large distances
Arboreal	Species that spend the majority of their time in trees
Semiaquatic	Species with the ability to live on land and in the water
Aquatic	Species that spend the most of their time in water
Perch	Species that spend the most of their time perched
Walk	Species primary locomotion is done on the ground
Swim/Walk	Species that spend most of the time walking and swimming

Phylogenetic Tree

Due to the large diversity of individuals within this study, a customized phylogenetic tree was created using the National Center for Biotechnology Information (NCBI) taxonomy based phylogenetic tree generator phyloT (Ciccarelli et al., 2006; An et al., 2016; Fu et al., 2017). Visualization of the phylogenetic tree uses an open source tree visualization tool called iTOL (Letunic & Bork, 2006, 2011, 2016). Free access is made possible through funding from the European Molecular Biology Laboratory and Biobyte Solutions. Through the iTOL tool, specific study-based customizations such as pruning of branches, color assignments, and formatting can be carried out. The tree was created in the newick format making it compatible with the Geomorph library in R (Adams & Otarola-Castillo, 2013; R Core Team, 2014).

Categorizing Unknowns

PCA scores were converted to basic meristic ratios to allow comparison of new specimens not included in the original PCA. These new specimens serve as "unknown" individuals to be compared with the VZAP specimens. The ratios measured consist of the most important shape variation described by PC1 and PC2. The ratio for PC1 of the femora is a length to distal width ratio and the ratio for PC2 of the femora is a distal width to distal depth ratio (Fig. 2.3). The ratio for PC1 of the humeri is a length to distal width ratio and the ratio for PC2 is a proximal depth to proximal width ratio (Fig. 2.4).

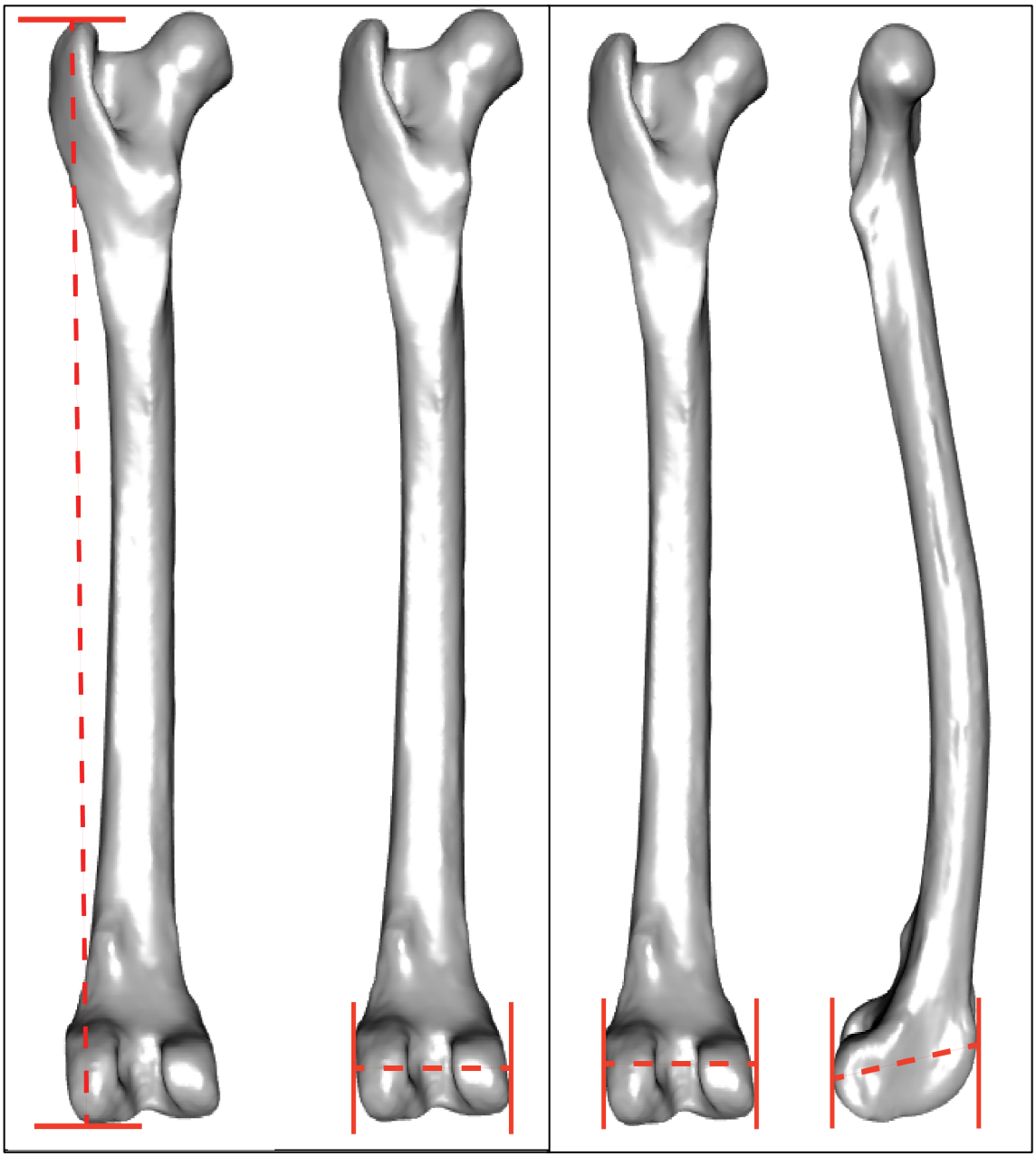

Figure 2.3. Measurements of the femur used to create the ratios for the meristic analysis. Each measurement represents the major shape variation described by PC1 and PC2. Measurements for PC1 create a height to width ratio (left). Measurements for PC2 create a width to depth ratio (right).

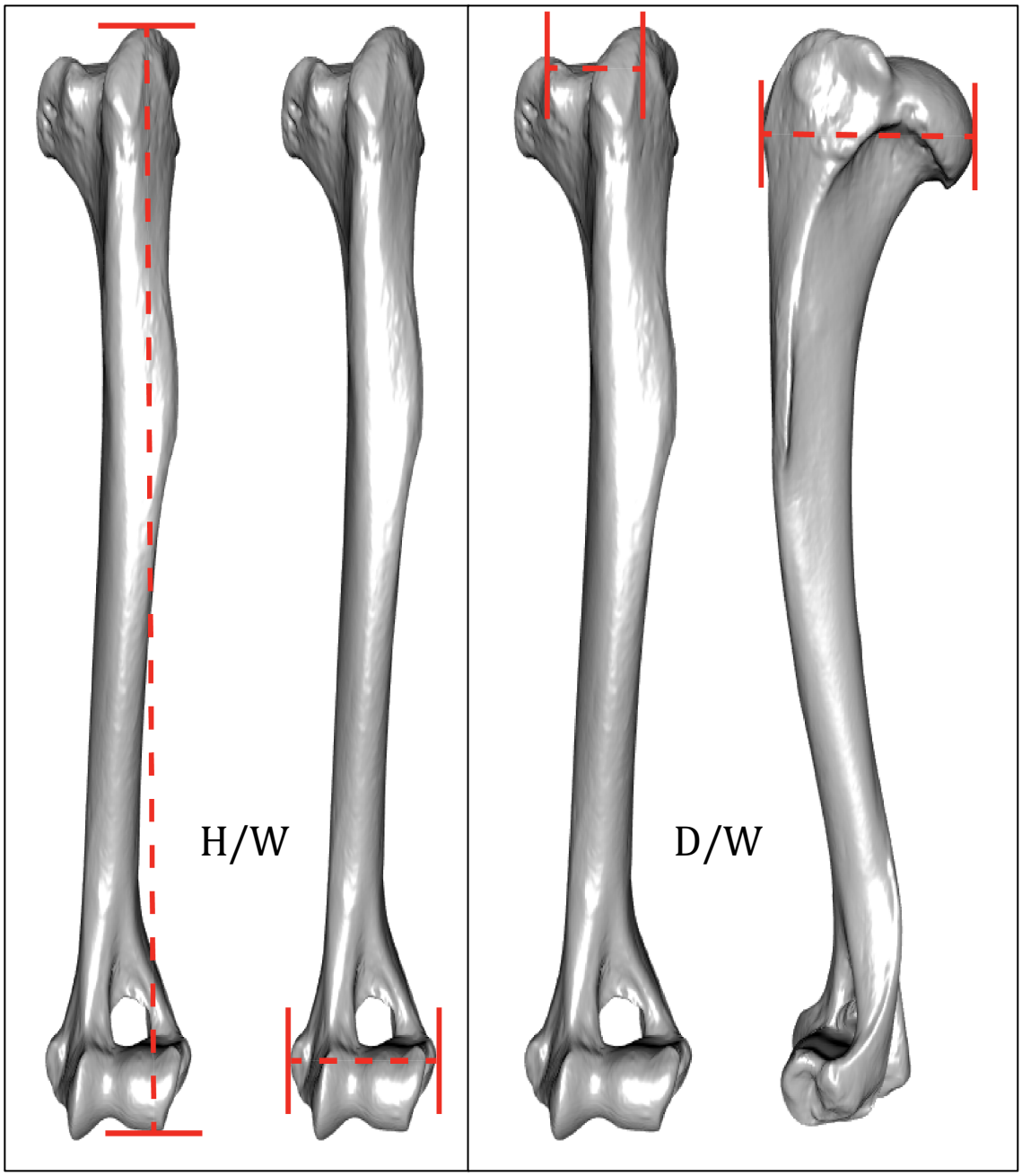

Figure 2.4. Measurements of the humerus used to create the ratios for the meristic analysis. Each measurement represents the major shape variation described by PC1 and PC2. Measurements for PC1 create a height to width ratio (left). Measurements for PC2 create a depth to width ratio (right).

3. RESULTS:

Landmark Analysis

There is a balance between the landmark quantity and variance. Too few landmarks oversimplify a complex shape, but it is easy to administer, and more easily allows for homologous-only landmarks. Too many landmarks reduce the significance of PC1, however this captures a more accurate representation of shape variation.

Compared to the 250, 500 and 1,500-sliding landmark methods, the 50-sliding landmark method consisted of a larger eigenvalue for PC1 (Fig. 3.5). The 50-sliding landmark method also consisted of the lowest amount of locomotor groups that overlapped as well as the lowest amount of total overlap seen among groupings compared to the 250, 500 and 1,500-sliding landmark methods (Fig. 3.6).

A comparison between the 7-fixed method and the 50-sliding landmark method showed a higher PC1 eigenvalue for the 7-fixed method (Fig. 3.5). The 50-sliding landmark method however, resulted in a lower number of overlapping locomotor groups and a lower amount of total overlap among groups (Fig. 3.6). The total area of the locomotor groups is also decreased in the 50-sliding method, indicating more tightly clustered groupings within the PCA morphospace (Fig. 3.7).

A 50-sliding landmark method resulted in the most distinct groupings of phylogeny and functionality and therefore, is the most appropriate method for the specimens of this study. The quantity of 50-sliding landmarks proved to be a better quantity used over 250, 500 and 1,500 landmarks because the 50-landmark tests resulted in lower number of locomotor group overlap and the lowest amount of total overlap. The 50-sliding landmark method was then compared to a 7-fixed landmark method. The PCA

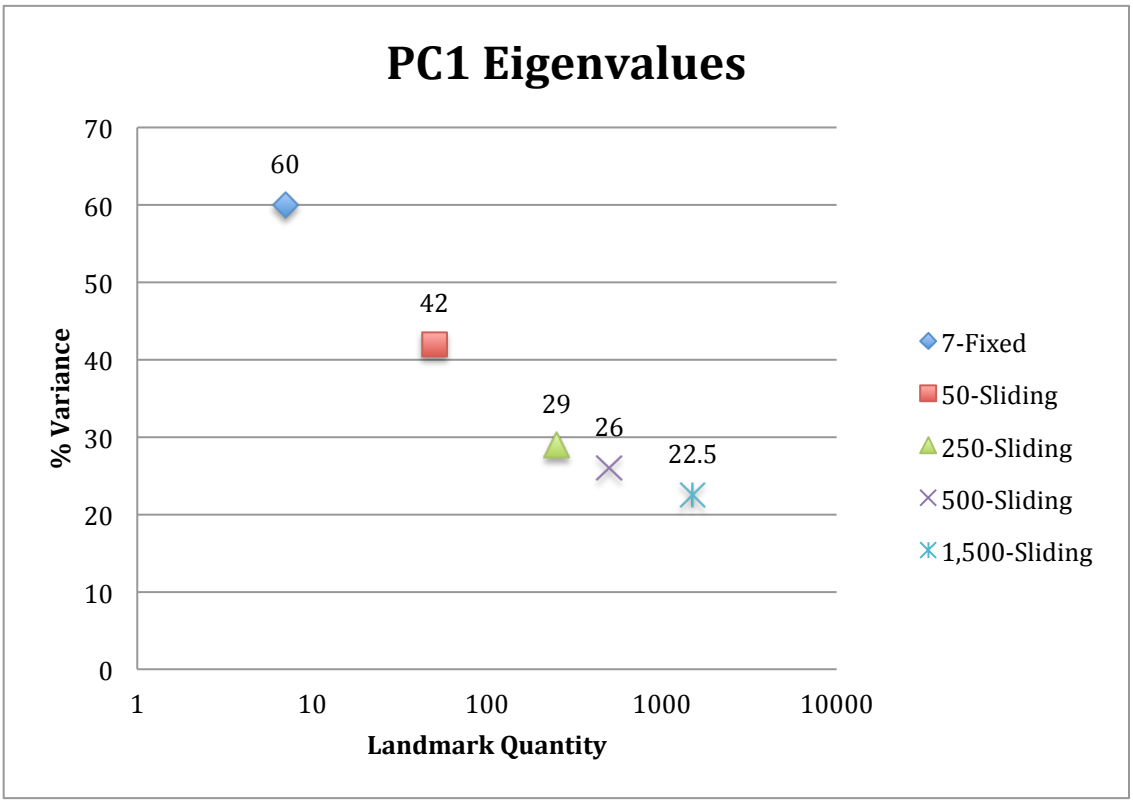

Fig. 3.5. Eigenvalue results comparing the percent of variance seen for PC1 for 7-fixed, 50, 250, 500 and 1,500-sliding landmark methods

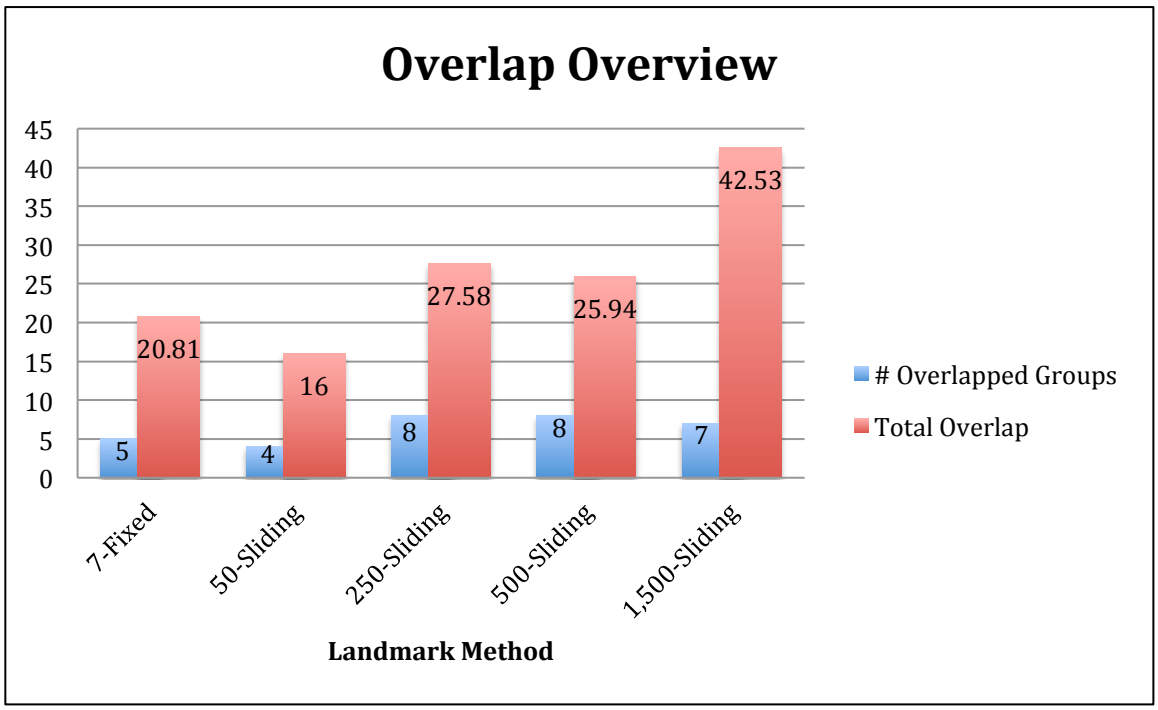

Fig. 3.6. Comparison between landmark methods and the total number of groups overlapped and total overlap seen between groups plotted in the PCA.

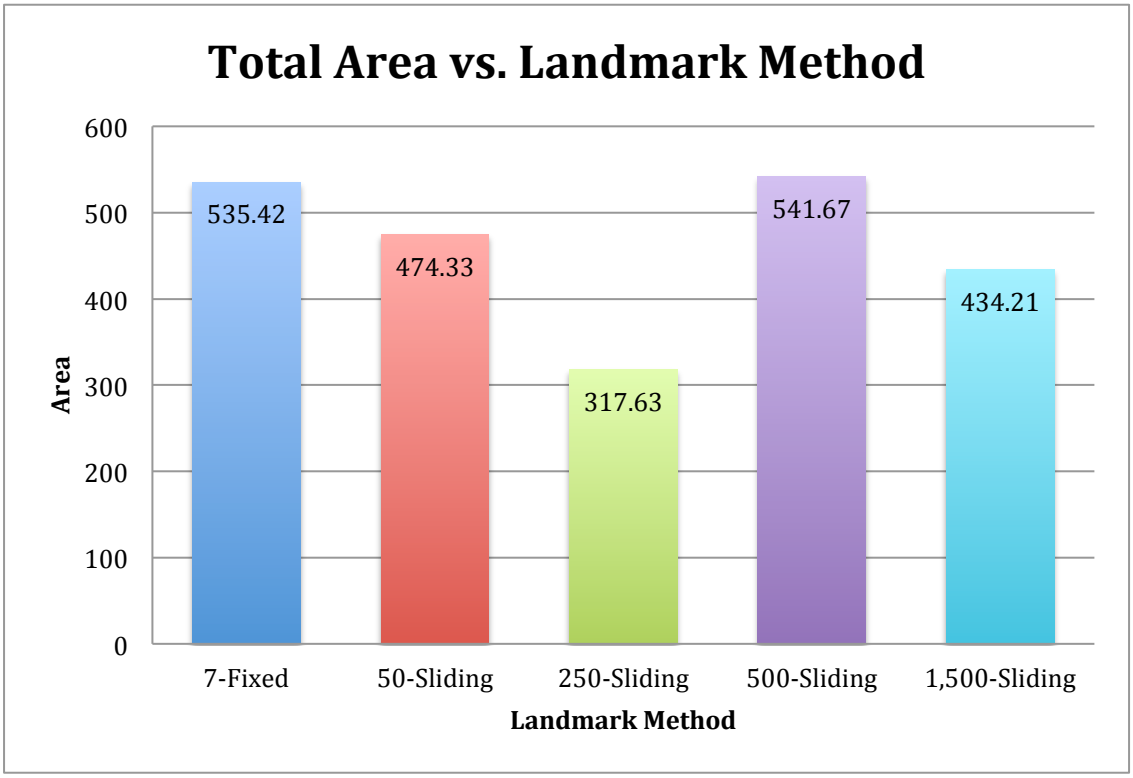

Fig. 3.7. Comparison between landmark methods and total area of groups within the PCA.

plot for each looked very similar, however, the 50-sliding landmark resulted in fewer groups overlapped, a lower amount of total overlap and a lower total area of the locomotor groups within the morphospace. Another major factor when determining between the 7-fixed and the 50-sliding methods was the ability to see shape variations of both the femora and humeri that cannot be seen with the 7-fixed results. TPS grids and vector deformation grids both identify the fundamental shape variation of PC1, however, the 50-sliding method captures variation seen over the surface of the entire bone. Variations such as the robustness of trochanters and other important muscle attachments can be captured using a 50-landmark method. These results and the ability to analyze the shape variation of these muscle attachments play a key role when analyzing functionality of the specimens of this study. The 50-sliding landmark method therefore, meets the landmark method criteria and can provide a PCA with more distinct groupings of phylogeny and functionality, which is one of the main goals of this study. Given these observations, the remainder of the study will focus on a 50-sliding landmark method.

Principle component analysis of the femora

The first two PCs of the PCA for the femora explained 52 percent of the total variance: 42 and 10 percent, respectively. The positive values of PC1 represent a femur that is short, wide and robust, whereas the positive values for PC2 represents a femur that has a deep patellar groove and robust medial and lateral condyles.

The phylogenetic categories are all distinct at all scales in the PCA. The groups are more distinct and tightly clustered within the morphospace with lower phylogenetic levels.

Class Mammalia and Aves showed clear differences between groups with positive PC1 and PC2 values (Fig. 3.8).

The order level showed distinct order groupings within the morphospace (Fig. 3.9). Mammalian orders Carnivora and Artiodactyla are distinctly separate from each other and distinctly separate from the Aves order groupings. The Aves order groupings show distinct clusters of specific orders, however, there is large overlap of the Aves orders with the exception of the order Gaviiformes, which form an isolated group.

The family level showed small distinct family groupings within the morphospace (Fig. 3.10). The mammalian family groupings are small and distinct and show very little overlap. The overlap only occurs with family Bovidae and Cervidae and family Mustelidae and Ursidae. The groupings of the Aves families show more overlap, however, the overlap has decreased greatly from the overlap seen when looking at the Aves order clusters.

Distinct groupings within the PCA are also true for function, which showed distinct locomotion groupings within the morphospace (Fig. 3.11). Aquatic locomotor habits, with positive values for PC1, are clearly different than a walking locomotor habit. The cursorial locomotor habit plots around the mean of PC1 and is distinctly separate from an aquatic locomotor habit. Between the aquatic and cursorial locomotor habits lies the intermediate semiaquatic locomotor habit. The superposition of PCA plots for phylogeny and function displayed phylogenetic groups that can be separated into smaller groupings by locomotor habits.

At the class level, class Mammalia can be distinctly separated into four locomotor groupings, cursorial, arboreal, aquatic and semiaquatic. At the order level, the Carnivora

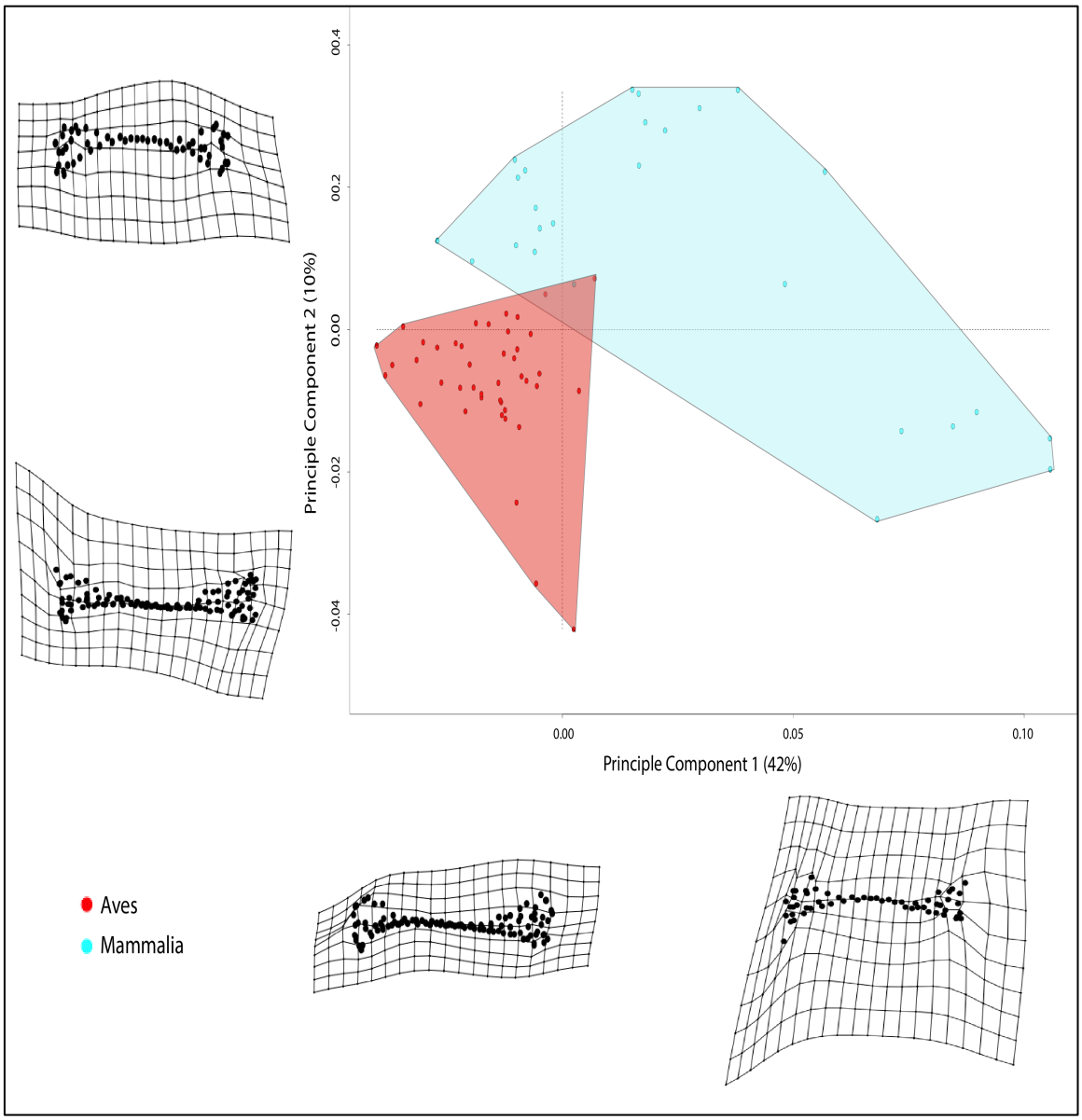

Fig. 3.8. PCA of the femora for PC1 (42%) and PC2 (10%) showing the distribution of class groups within the morphospace. Shape change along each axis are shown in thin-plate spline deformation grids.

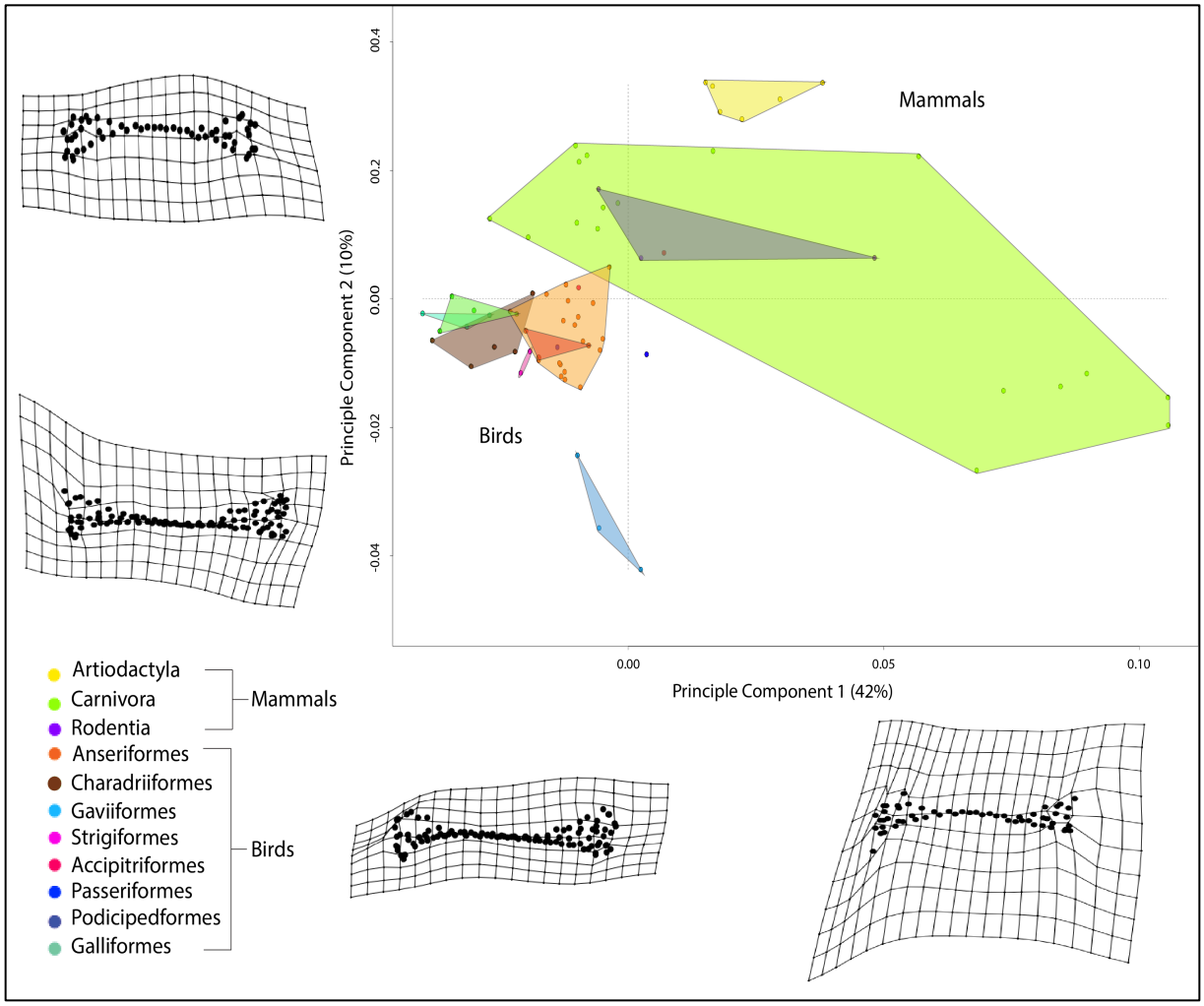

Fig. 3.9. PCA of the femora for PC1 (42%) and PC2 (10%) showing the distribution of order groups within the morphospace. Shape changes along each axis are shown in thin-plate spline deformation grids.

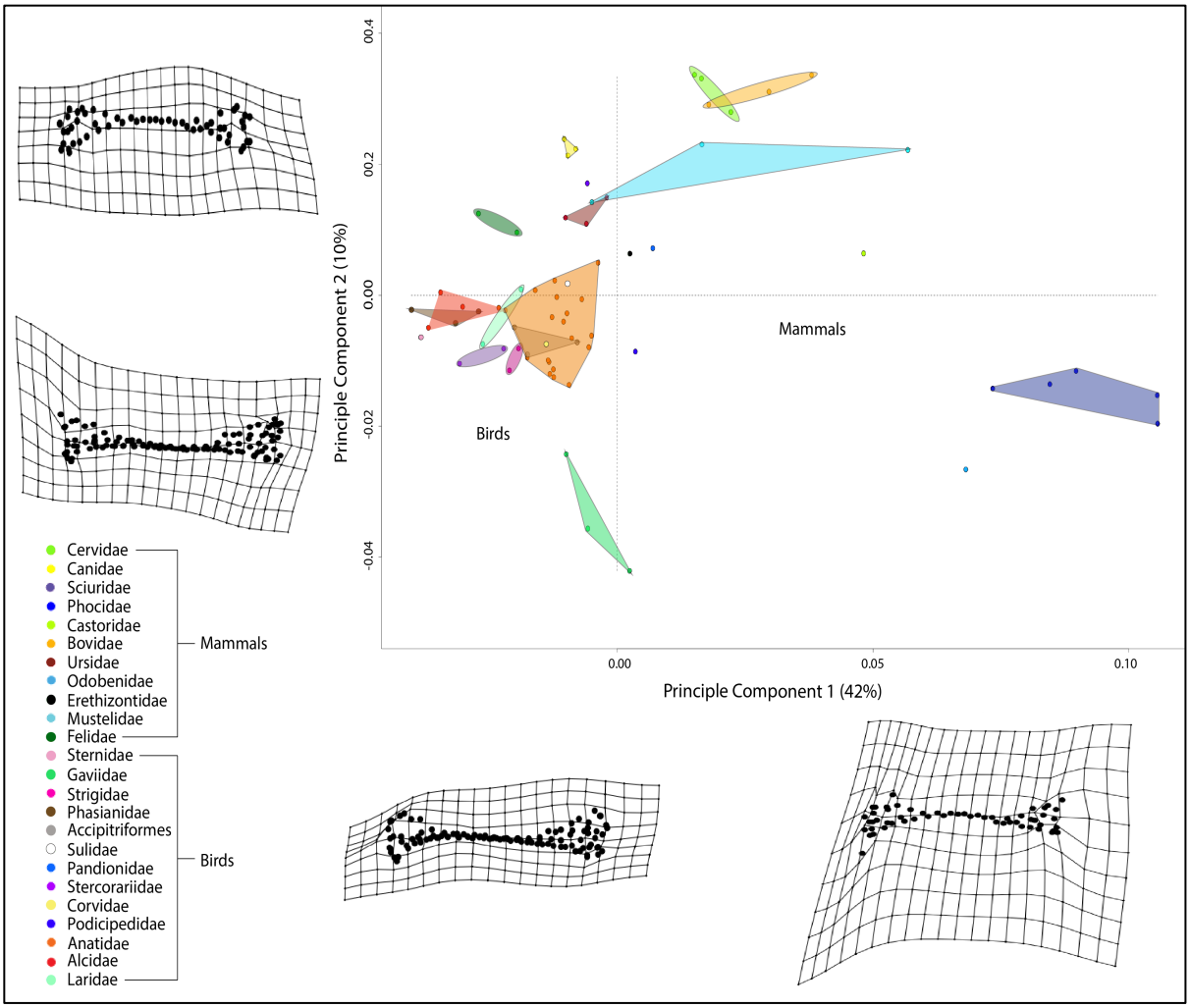

Fig. 3.10. PCA of the femora for PC1 (42%) and PC2 (10%) showing the distribution of family groups within the morphospace. Shape changes along each axis are shown in thin-plate spline deformation grids.

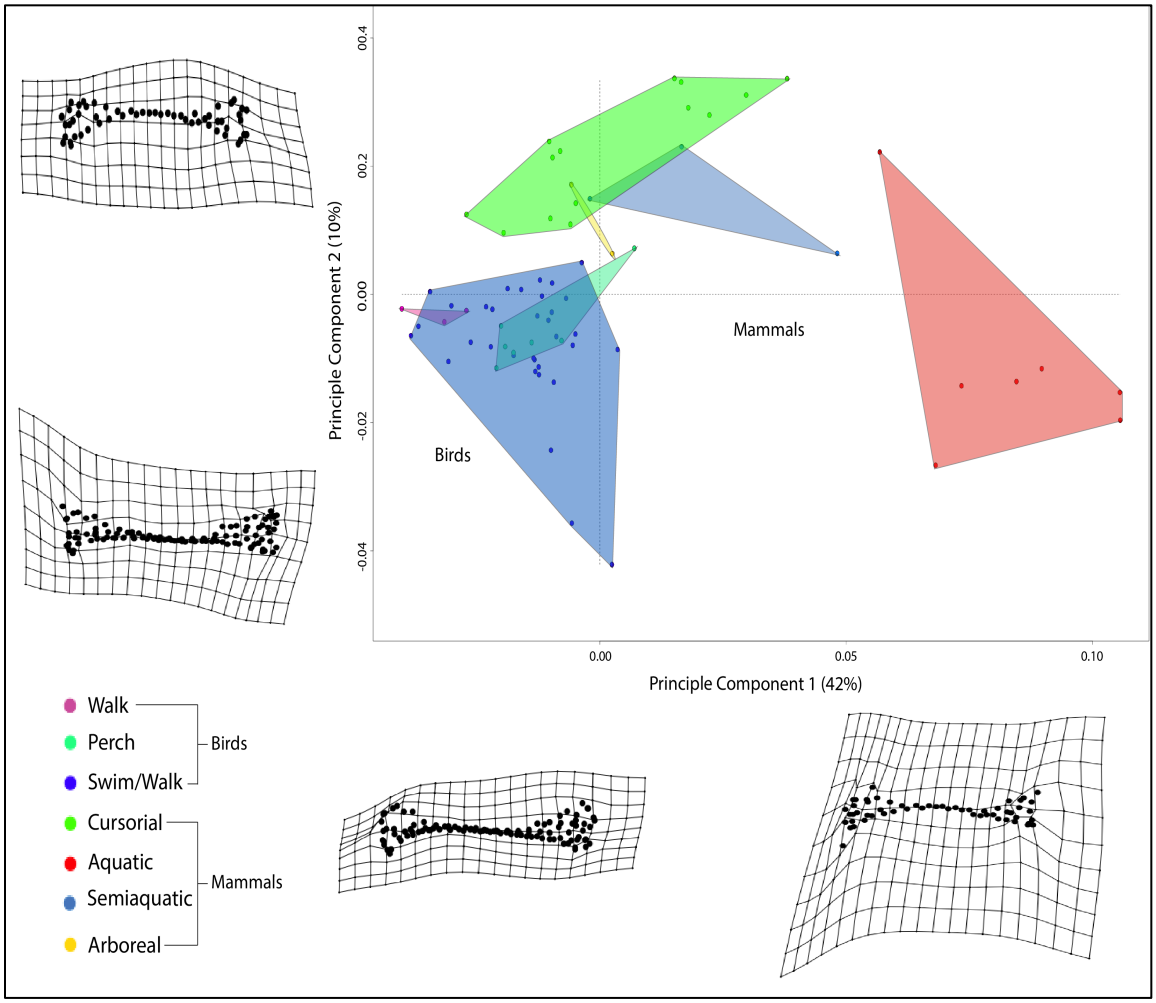

Fig. 3.11. PCA of the femora for PC1 (42%) and PC2 (10%) showing the distribution of locomotion groups within the morphospace. Shape changes along each axis are shown in thin-plate spline deformation grids.

order can be separated into two distinct locomotor groups, aquatic carnivores and terrestrial carnivores.

Principle component analysis of the humeri

The first two PCs of the PCA for the humeri explained 65 percent of the total variance: 59 and 6 percent, respectively. The positive values of PC1 represent a humerus that is compressed and robust. The positive values of PC2 represent a humerus that consists of a large humeral head that extends caudally, a lesser tubercle that shifts laterally and a greater tubercle that shifts medially.

The phylogenetic categories are all distinct at all scales in the PCA. The groups become more distinct and tightly clustered within the morphospace with lower phylogenetic levels.

Class Mammalia and Aves showed clear differences between groups along the PC1 axis and the separation of classes are more distinct than the femora results (Fig. 3.12).

The order level showed distinct order groupings within the morphospace (Fig. 3.13). The Mammalian orders are overlapped for PC1 but show distinct differences for PC2. The Aves show small order clusters that are distinctly different than the Mammalian orders with negative PC1 values and large overlap among the orders with exception of the Galliformes.

The family level showed distinct family groupings within the morphospace (Fig. 3.14). The Mammalian families, with positive values for PC1, show little to no overlap among families. The Aves family clusters are smaller than the Aves order clusters and there is more distinct separation among families.

Distinct groupings within the PCA are also true for function, which showed distinct locomotion groupings within the morphospace. The locomotor habits showed distinct locomotion groupings within the morphospace (Fig. 3.15). Mammalian cursorial locomotor habit overlapped for PC1 with aquatic, semiaquatic, and arboreal habits, but showed a significant difference for PC2. The Aves showed the elliptical locomotor habit distinctly separate from the dynamic soaring habit for PC1.

Similar to the femora PCA plots, the superposition of the phylogeny and function PCA plots for the humeri displayed phylogenetic groups that can be separated into smaller distinct locomotor groupings. At the class level, class Mammalia can be distinctly separated into four locomotor groupings, cursorial, arboreal, aquatic and semiaquatic. At the order level, the Carnivora order can be separated into two distinct locomotor groups, aquatic carnivores and terrestrial carnivores.

Categorizing Unknowns

Femora

Each femur PC score within the morphospace of the PCA was converted into a meristic ratio (Fig. 3.16; Appendix VI). Measurements taken for these ratios represent the major shape change seen along each PC axis. For the femur, a length to width (L/W) measurement was taken and correlates to an R^2 value of 0.79. The maximum PC1 value seen within the morphospace has a L/W ratio of approximately 1.65 and represents an aquatic locomotor habit. The minimum PC1 value seen within the morphospace has a L/W ratio of approximately 6.40 and represents a walking locomotor habit. The femora are more compressed and robust when moving along the PC1 axis in the positive

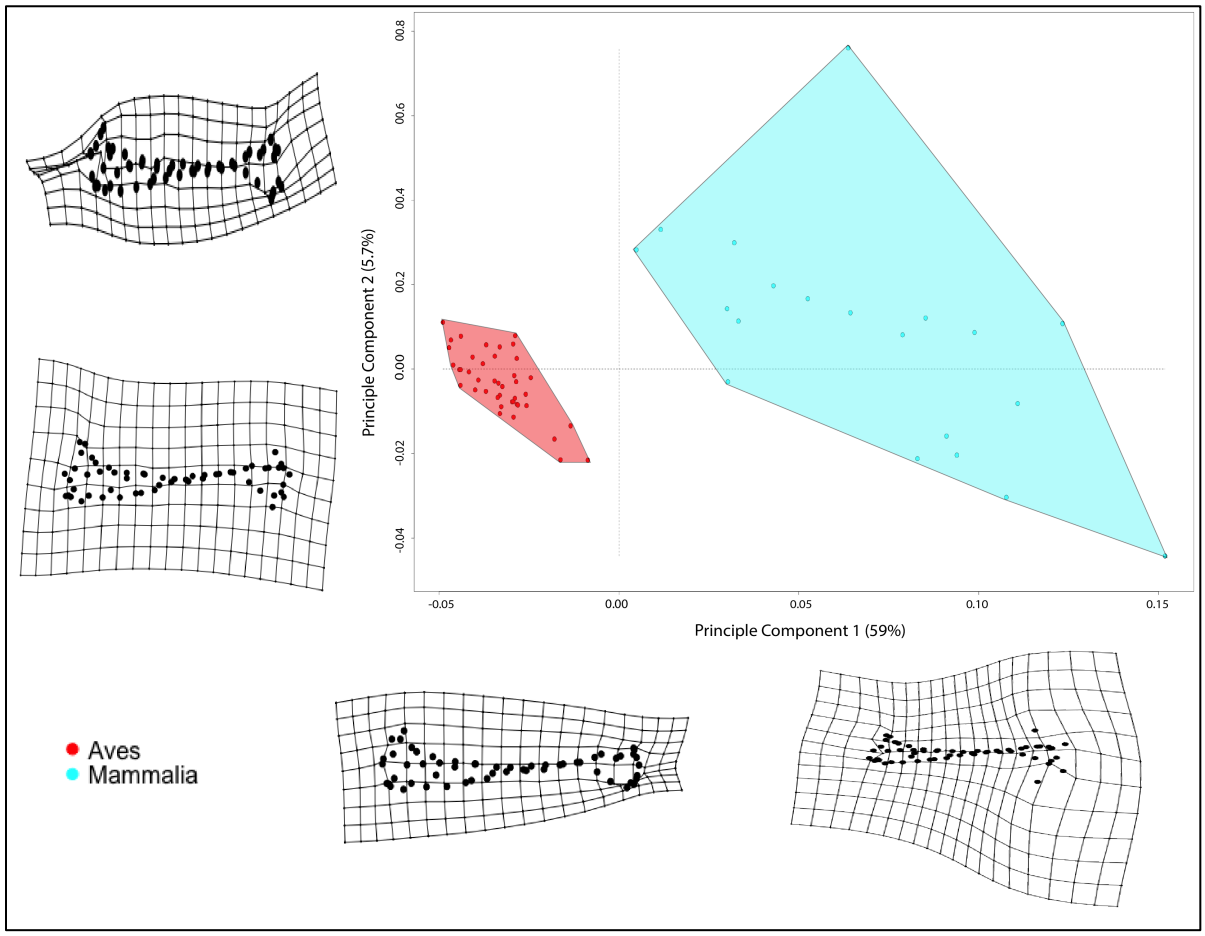

Fig. 3.12. PCA of the humeri for PC1 (42%) and PC2 (10%) showing the distribution of class groups within the morphospace. Shape changes along each axis are shown in thin-plate spline deformation grids.

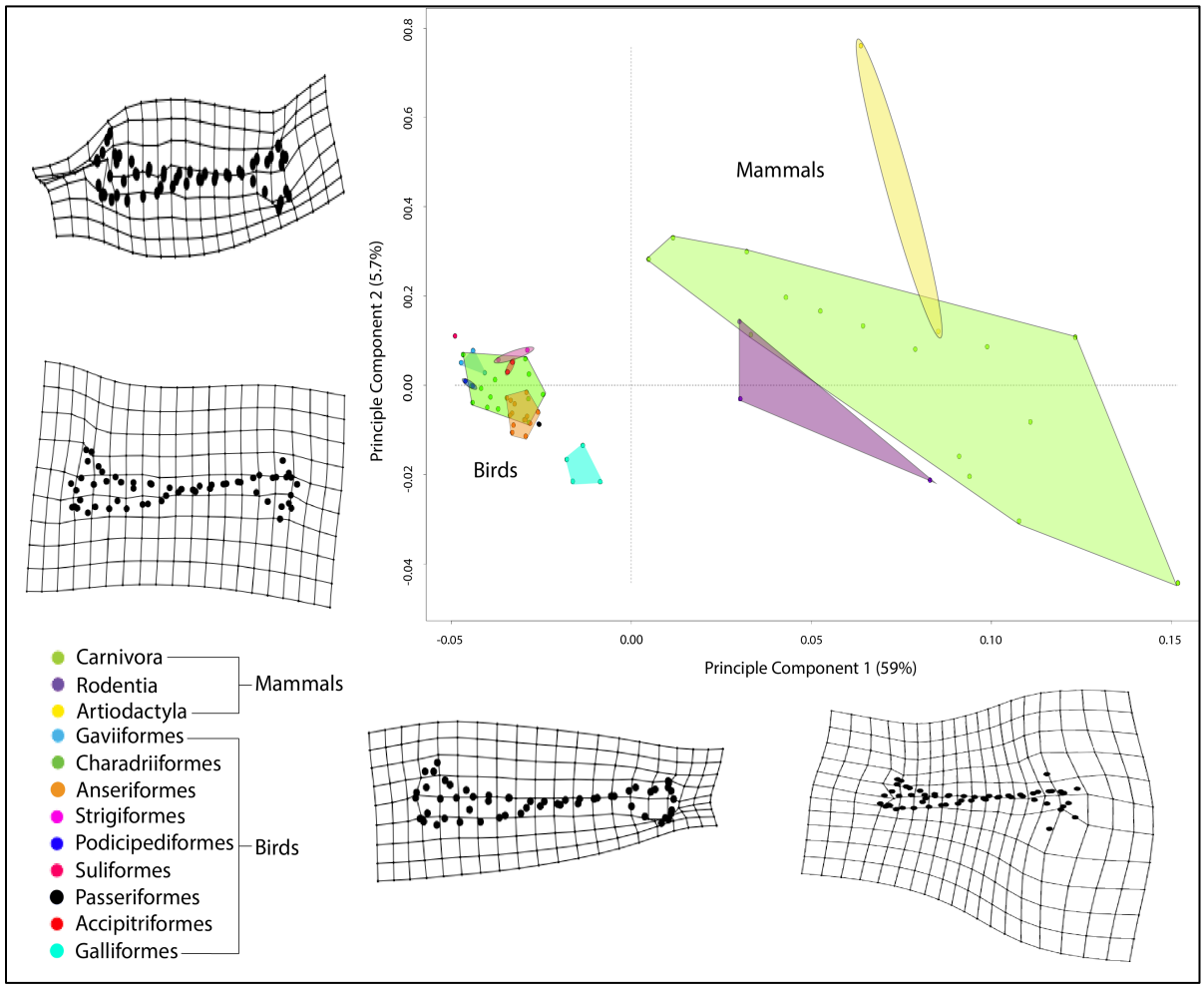

Fig. 3.13. PCA of the humeri for PC1 (42%) and PC2 (10%) showing the distribution of order groups within the morphospace. Shape changes along each axis are shown in thin-plate spline deformation grids.

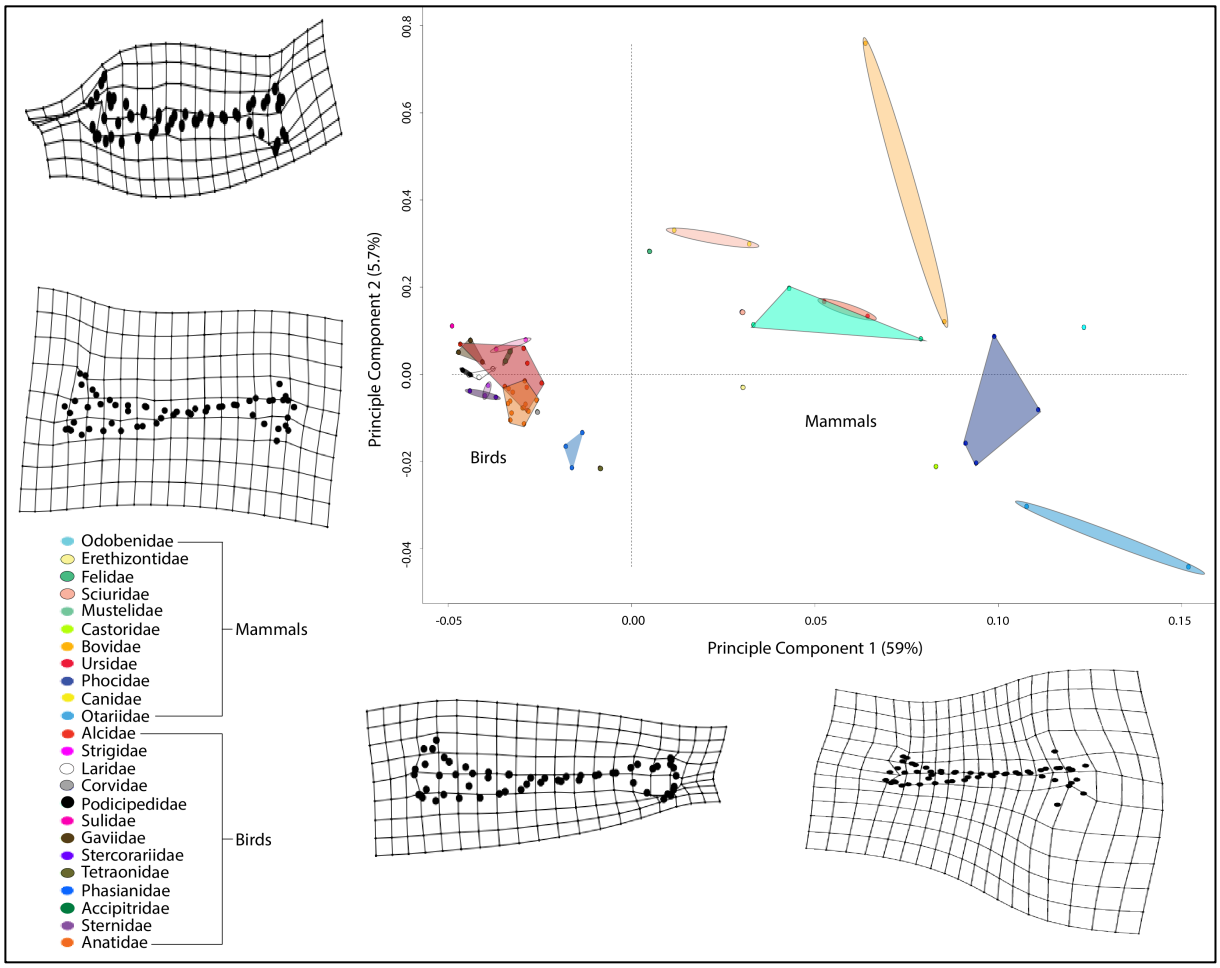

Fig. 3.14. PCA of the humeri for PC1 (42%) and PC2 (10%) showing the distribution of class groups within the morphospace. Shape changes along each axis are shown in thin-plate spline deformation grids.

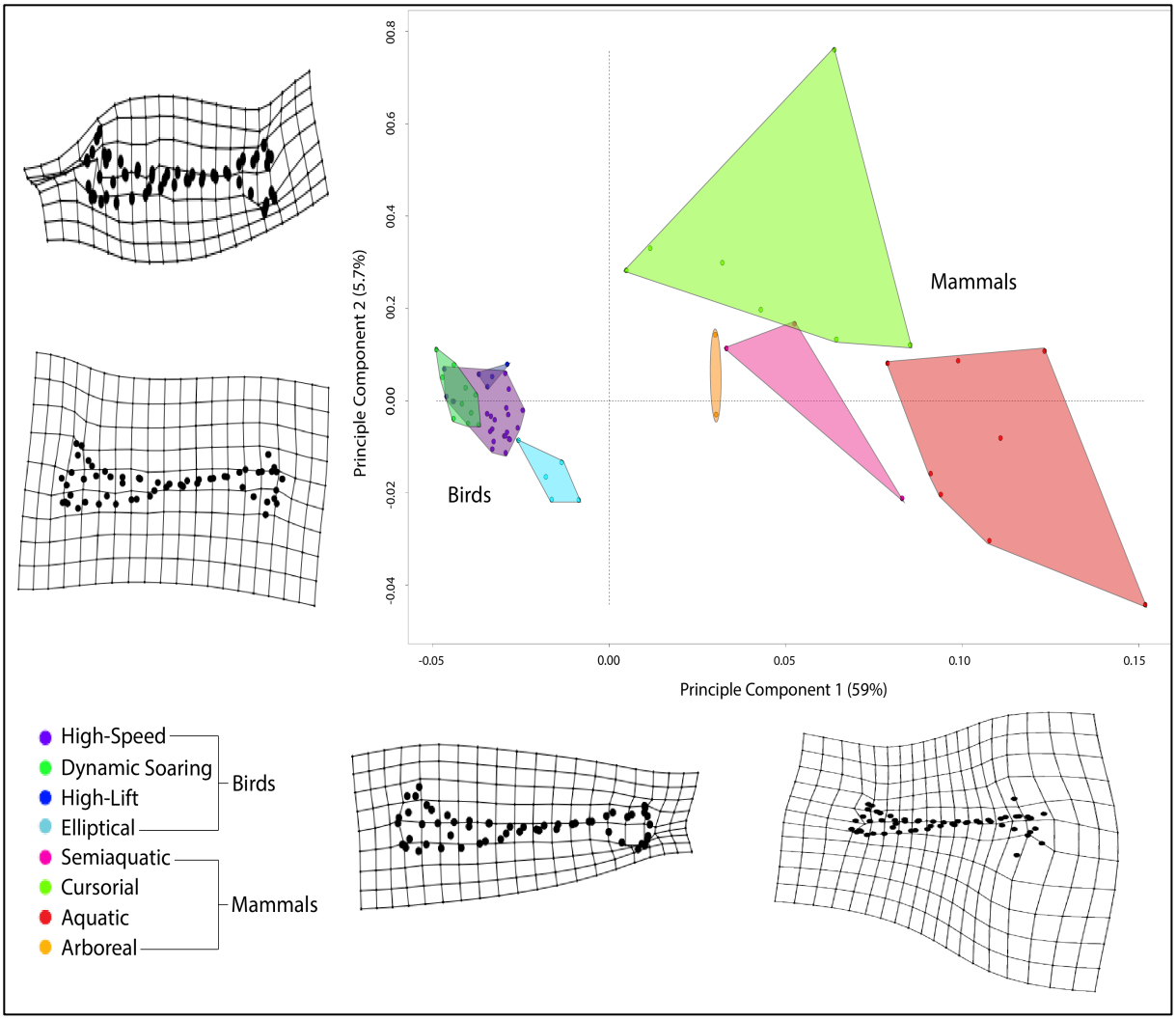

Fig. 3.15. PCA of the humeri for PC1 (42%) and PC2 (10%) showing the distribution of class groups within the morphospace. Shape changes along each axis are shown in thin-plate spline deformation grids.

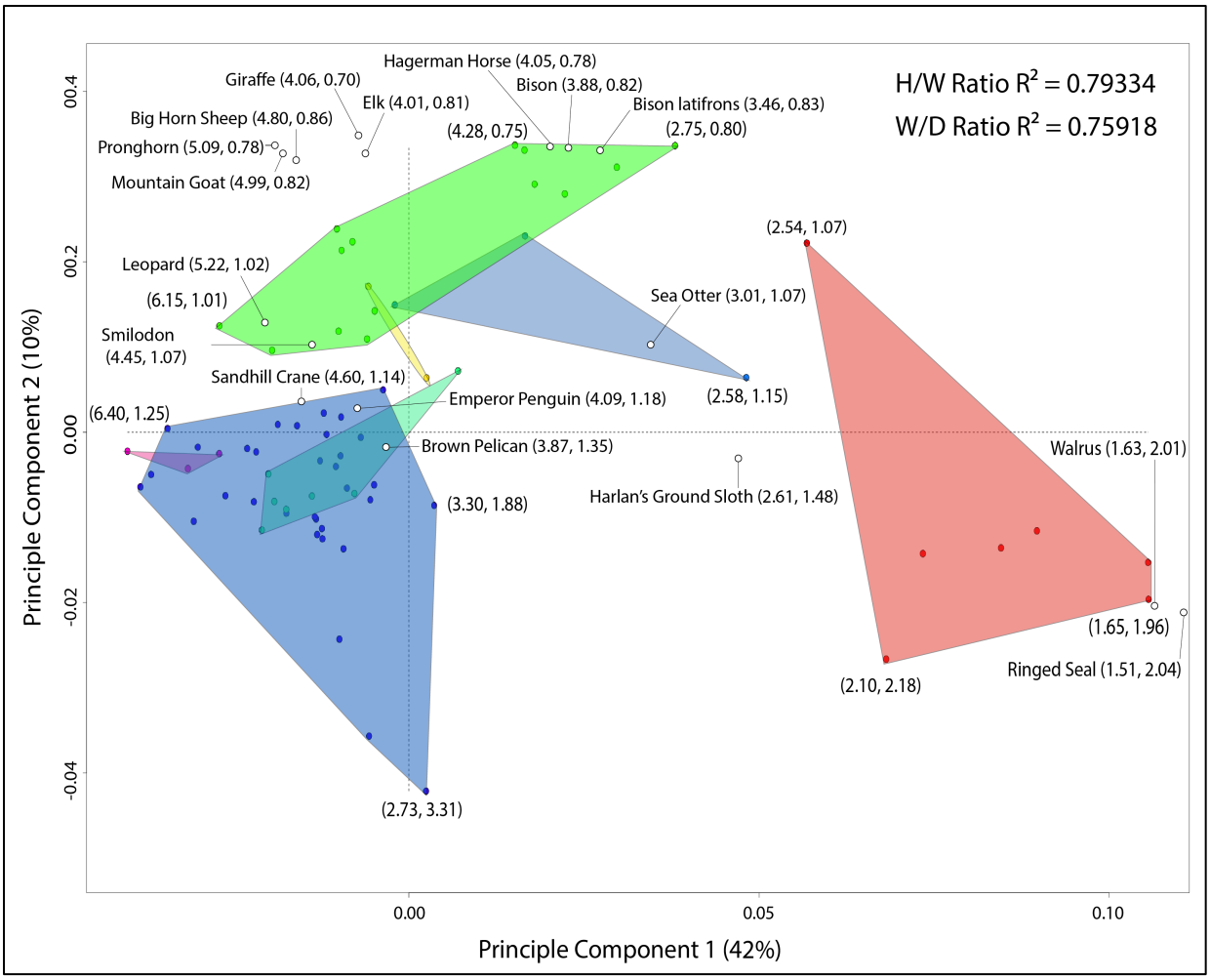

Fig. 3.16. Results of the meristic analysis of the femora. PC1 and PC2 scores of the PCA are converted into meristic ratios. An additional 17 femora ratios from outside the original dataset were plotted within the PCA morphospace, each plotting within the appropriate locomotor group.

locomotor habit. The maximum PC2 value has a W/D ratio of approximately 0.75 and represents a cursorial direction. Ratios for the PC1 axis separate aquatic locomotor habits from cursorial, semiaquatic, arboreal, walking, swim/walk and perching locomotor habits.

The measurement for PC2 that describes the major shape change seen within the morphospace is a width to depth (W/D) ratio and correlates to an R^2 value of 0.76. The minimum PC2 value has a W/D ratio of approximately 3.30 and represents a swim/walk locomotor habit. Ratios for the PC2 axis separate the cursorial and semiaquatic locomotor habits from the walking, perching and swim/walk locomotor habits.

There were 17 additional femora measurements taken of specimens outside of the original dataset. Each of the ratios from these femora fell within the appropriate locomotor habit. The additional specimens also plotted closely to specimens of similar orders and families, for example, Felids, such as the Smilodon and leopard, plot closely to the bobcat and mountain lion ratios; and Artiodactyls, such as the big horn sheep, mountain goat and pronghorn are all closely plotted together within the morphospace.

Humeri

Each humeri PC score within the morphospace of the PCA was converted into a meristic ratio (Fig. 3.17; Appendix V). The PC1 axis for the humeri is described by a length to width (L/W) ratio and correlates to an R^2 value of 0.75. The maximum value of PC1 is approximately 2.25 and represents an aquatic locomotor habit. The minimum value of PC1 is approximately 10.42 and represents a dynamic soaring locomotor habit. The PC1 ratio values show significant differences between the aquatic, semiaquatic, cursorial and arboreal locomotor habits and the elliptical, high-lift, high-speed and

dynamic soaring habits. Lower ratio values show overlap between the cursorial and the arboreal, semiaquatic and aquatic locomotor habits. These locomotor habits are distinctly separated by the PC2 ratio values. The PC2 ratio values are obtained through a depth to width (D/W) measurement that correlates to an R^2 value of 0.86. The maximum PC2 ratio value is approximately 3.02 and represents a cursorial locomotor habit. The minimum PC2 ratio value is approximately 1.20 and represents the semiaquatic locomotor habit. The PC2 ratios distinctly separate the cursorial locomotor habit from the arboreal and the semiaquatic locomotor habits.

An additional 15 humeri were measured from specimens outside the original dataset. Each L/W and D/W ratio value for all the additional humeri fell within the appropriate locomotor habit. Similar to the femora, these additional specimens also plotted near similar specimens of the same order and family within the morphospace. For example, the bison and bighorn sheep have high D/W ratios, plotting within the cursorial locomotor habit and close to other Artiodactyl specimens.

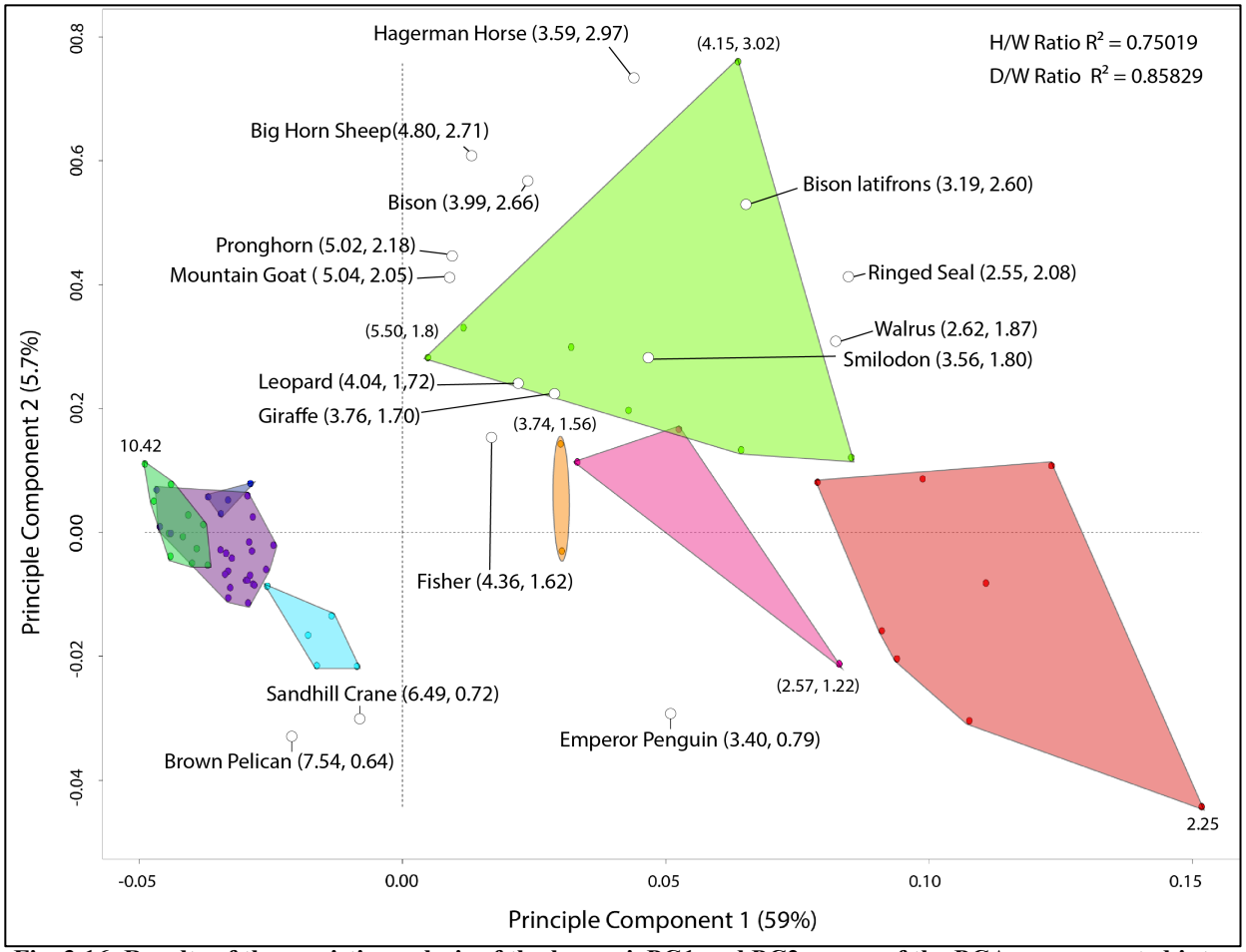

Fig. 3.16. Results of the meristic analysis of the humeri. PC1 and PC2 scores of the PCA are converted into meristic ratios. An additional 17 femora ratios from outside the original dataset were plotted within the PCA morphospace, each plotting within the appropriate locomotor group.

4. DISCUSSION:

Principle Component Analysis

Overview

The PCA results show what was to be expected with phylogeny and functionality playing important roles for shape variation among the individuals of this study. This is shown for both the femur and humerus bones. On the PCA scatterplots at the species level, there consists of no overlap among individual species. This separation of shape variation continues at multiple levels (family, order, class) and is observed at the largest level of this study in class, indicating that phylogeny plays a large role in shape variation. Within locomotor groups, individuals that swim tend toward the positive end of PC1. This is observed in mammals, with the semiaquatic mammals pushed toward more positive PC1 scores compared to terrestrial mammals. Aves also show this restriction with the femora of birds that swim and dive. They are distributed within their phylogenetic groups but tend toward a positive PC1 value and the aquatic locomotor habit. These results indicate that bone shape of these individuals is intermediate between aquatic form and terrestrial form within the constraint of phylogeny.

The effects of locomotion also play important roles in shape variation. The order Carnivora is widely distributed on the PCA scatterplots. This large grouping decreases into smaller groupings of locomotion. Aquatic carnivores and terrestrial carnivores are completely separated. The shape variation driven by locomotion can also be observed at the class level. There is a large distribution of the Mammalia class, but it can be divided into smaller clustered locomotor groups of aquatic and terrestrial mammals. Dividing

larger phylogenetic groupings into smaller groupings based on locomotor habits verifies that locomotion also plays an important role for shape variation among individuals.

Principle component analysis of humeri

A positive PC1 represents a humerus that is short and stout. The greater tubercle and deltoid tuberosity are elongated distally down the shaft. The greater tubercle is also more robust at the distal end. The head elongates in the caudal direction and is more spherical. The medial epicondyle shifts in the medial and proximal direction and the lateral epicondyle shifts in the lateral and proximal direction. The trochlea increases in the distal direction and shifts in the medial direction and the capitulum also increases in the distal direction and shifts in the lateral direction. Overall, a positive PC1 value represents a humerus that is short, stout and has a head that is increased in the caudal direction.

A positive PC2 value represents a humerus with the caudal apex of head increased in the caudal direction and shifted distally. The lesser tubercle increases in the proximal direction and shifts laterally. The greater tubercle and deltoid tuberosity shifts medially. The apex of the medial epicondyle shifts in the cranial direction and the apex of the lateral epicondyle shifts in the caudal direction.

The locomotor groups of the humeri are primarily determined by variation of shape described by PC1. This variation completely separates the aquatic mammals from the Aves. The semiaquatic group is an intermediate group, overlapping both the terrestrial mammals and aquatic mammals. The terrestrial mammals, including the cursorial and arboreal locomotion habits, fall in between the aquatic mammals and the Aves on the scatterplot along the PC1 axis.

The major shape variation of the aquatic species is determined by a positive PC1 value and consists of humeri that are short and stout. The head elongates in the caudal direction and is more spherical. The elongation and spherical shape of the head provides greater range of motion of flexion, extension, and rotation of the limb (Leach, 1961). The greater tubercle and deltoid tuberosity are elongated distally down the shaft. The greater tubercle is the primary insertion point for major muscles of extension and flexion of the humerus helping to thrust the limb for swimming. These muscles include the supraspinatus, pectoralis profundus and the pectoralis superficialis. The deltoid tuberosity is the attachment for the deltoideus muscle, which is also a major muscle used for flexion and abduction of the humerus during swimming (Miller et al., 1964). The medial and lateral epicondyles are enlarged and extend medially and laterally respectively. These are attachment points for common extensor and flexor muscles of the forearm and carpals of the limb, which also supports swimming (Hildebrand, 1974; Hildebrand & Goslow, 2001; Polly, 2007; Samuels & Valkenburgh, 2008; Fabre et al., 2015). The trochlea and capitulum extends distally and articulate to the ulna and radius of the forelimb (Miller et al., 1964).

The distinct grouping of the cursorial locomotion group is driven by a positive PC2 value. The increased surface area of the greater tubercle and deltoid tuberosity and the decreased size of the lesser tubercle is consistent with previous studies stating that the bulk of the muscle attachment is near the proximal end of the femur to increase speed while reduction of the cost of energy (McGowan, 1999). The greater tubercle and deltoid tuberosity are the attachment points for the major flexion and extensor muscles of the humeri as stated above. The decrease of the lesser tubercle decreases the attachment and

size of the subscapularis, which primarily adducts the humerus (Miller et al., 1964). An increase in the size of the extensor and flexor muscles and a decrease in the adductor and abductor muscles in the cursorial mammals restricts the movement of the limbs to the line of direction of locomotion. The elongation of the trochlea and capitulum creates a larger hinge-like structure that articulates with the trochlear notch of the ulna that also reduces adduction and abduction of the forelimb and keeps the movement in the line of direction of locomotion (Hildebrand, 1974; McGowan, 1999; Polly, 2007).

The semiaquatic species are represented by positive PC1 values overlapping both the terrestrial and aquatic mammals. This shows that the semiaquatic species posses humeri with a mean shape that consists of characteristics of both the terrestrial and aquatic species. These characteristics consist of a robust proximal end including a robust greater and lesser tubercle, which increases the attachment points for flexor, extension, adduction and abduction muscles used in locomotion, increasing the strength and ability to swim (Hildebrand, 1974; Samuels et al., 2008).

The humeri in Aves is relatively similar for each of the locomotor habits and is determined by not only the locomotor habit, but also the size and weight of the bird (Gilbert et al., 1981; King & McLelland, 1985). The shape variation mainly consists of increased muscle attachments. The humeri for the Aves consist of negative PC1 values representing a humerus with a robust greater tubercle, robust deltoid crest at the proximal end and a head that is robust and flattened. The greater tubercle or pectoral crest in Aves is the attachment point for the pectoralis, which depresses the humerus and is the main muscle used for the downstroke of the wing (King & McLelland, 1985). The downstroke of the wing is the main driver of flight. This robust pectoral crest is also the attachment

point for the supracoracoideus muscle, which is attached on the opposite side from the pectoralis and is the main muscle used for the upstroke of the wing. The robust deltoid crest is the attachment point for the deltoideus major and deltoideus minor, which are the main muscles used for retraction and protraction of the humerus (Gilbert et al., 1981; King & McLelland, 1985). The negative apex of the PC1 axis consists of birds with dynamic soaring and high-lift wing habits. These are larger birds in size and therefore, need a humerus with large muscle attachments to increase muscle size capable of producing enough thrust for flight and the ability to abduct the humerus for long periods of time while gliding (Hildebrand, 1974; McGowan, 1999; Dial, 2003). The increased size and flattening of the head increases movement of the humerus in the dorsal and ventral direction, which is the upstroke and downstroke of the wing (King & McLelland, 1985).

Principle component analysis of femora

A positive PC1 value represents a femur that is short and stout. The greater trochanter is shifted laterally. The shaft becomes more robust and compressed and more curved in the cranial direction. The patellar surface is widened and the patellar groove becomes shallower. The distal apex of the lateral condyle shifts laterally and the distal apex of the medial condyle increases in the distal direction and shifts medially.

Shape variation for positive PC2 values of the femur consist of a greater trochanter that shifted medially and increased in the cranial direction. The femoral head's distal surface increases distally. The lateral surface of the shaft increases laterally. The medial condyle increases in the distal direction and the patellar surface decreases in width and becomes deeper.

Femoral shape for aquatic species is driven by positive PC1 values. Major shape variations seen in aquatic mammals are an enlarged greater trochanter, trochanteric fossa, intertrochanteric crest, and a decrease of the lesser trochanter. These are all muscle attachments for major extensor muscles of the femur including the gluteus medius, gluteus profundus, and the quadratus femoris, which drives the thrust of the hindlimb in swimming (Leach, 1961; Miller et al., 1964; Hildebrand, 1974; Hildebrand & Goslow, 2001; Polly, 2007; Samuels & Valkenburgh, 2008; Fabre et al., 2015).

The cursorial species are distinctly separate from other locomotor groups with positive PC1 and PC2 values. This mean shape is consistent with other studies for cursorial mammals and is described by a robust femur, a more robust and elongated greater trochanter and a deep patellar groove (Hildebrand, 1974; McGowan, 1999; Polly, 2007). The femur shape for cursorial mammals is ideal for running at high speeds. The elongated and robust trochanter provides a greater surface area for muscle attachments of larger muscles used for the extension of the femur as stated above. The bulk of the muscle attachments at the proximal end of the femur allows for a lever of extension of the limb and for traveling at higher speeds with less energy expenditure (Leach, 1961; Miller et al., 1964; Hildebrand, 1974; McGowan, 1999; Polly, 2007).

Femoral shape for arboreal species is driven by a negative PC1 value and a Positive PC2 value. This is consistent with previous studies and the major variables of mean shape include a more gracile greater trochanter, robust patellar surface, shallower patellar groove and a decrease in surface area of the lateral and medial epicondyles. The shallow and broad patellar groove of the femur increases climbing ability and flexibility of the hind limb. The decrease in size of the greater trochanter and the epicondyles allow

for the bone to be lighter and the animal more agile (Hildebrand, 1974; Hildebrand & Goslow, 2001; Samuels et al., 2008; Fabre et al., 2015).

The distribution of birds that swim/walk is large and plots with negative PC1 and PC2 values within the morphospace. The mean shape consists of a robust femur with a femoral head that is elongated and more robust. The robust femur allows for larger muscle attachments, which is important for muscle extension and flexion for birds that use their hind limb for thrust while swimming. The robust proximal end is important for landing as the femoral neck and greater trochanter absorb and compress the stresses of impact (Hildebrand, 1974; Gilbert et al., 1981; King & McLelland, 1985).

Femur mean shape for perching birds showing the most distinct distribution is driven by negative PC1 and PC2 values. Major shape variations include a more robust neck, head, greater trochanter and distal end. The robust neck and head act as a shock absorber while landing. The robust distal end also contributes to absorbing stresses and prevents over-protraction of the femur while landing. The pubo-ischio-femoralis inserts on the caudal surface of the distal femur and is the primary muscle for femoral retraction (Hildebrand, 1974; Gilbert et al., 1981; King & McLelland, 1985).

Femoral shape for walking birds is primarily driven by negative PC1 values. The greater trochanter shifts medially. The shaft becomes more gracile and the curvature of the shaft decreases. The distal apex of the lateral condyle shifts medially and the distal apex of the medial condyle shifts laterally. The condyles are muscle attachments for the gastrocnemius, which is used for extension of the tarsal joint and flexion of the knee (Hildebrand, 1974; Gilbert et al., 1981; King & McLelland 1985).

The PCA as discussed above showed expected results and indicates that phylogeny is important for bone shape. Distinct phylogenetic groupings on multiple scales are seen and at the lowest levels the phylogenies are isolated. The results for functionality also showed expected results. The locomotion groups all pull apart independent of phylogeny and intermediate groups such as semiaquatic plot in the appropriate locations within the morphospace.

Categorizing Unknowns

The PCA results for the locomotor groups are approximated using meristic variables. These results lead to the final aspect of the project. If specific locomotor groups can be categorized, can these PCA plots be used to determine an unknown specimen? The PC scores resulting from the PCA for each individual are converted into simple meristic ratios. The ratios chosen for PC1 and PC2 represent the largest shape variation observed along its axis. This analysis used specimens outside the original dataset to act as "unknown" individuals. These additional specimens consist of multiple phylogenetic levels, locomotor habits and are both extinct and extant specimens. Both the femora and humeri were measured and tested to determine if the unknown specimen plotted in the appropriate location within the morphospace. The results for both the femora and humeri were similar. The added ratios of unknown specimens not only plotted within their accurate locomotor group, but also plotted next to specimens of similar class, order and family. For example, specimens from the order Artiodactyla including mountain goat, pronghorn, and big horn sheep all plot near each other within the morphospace and within the appropriate cursorial locomotor group. Extinct and extant specimens at the same family level plot together as well. This is observed with the

family Bovidae and the extant species *Bison bison* and the extinct species *Bison latifrons*. The conversion back to a simple meristic ratio measurement not only makes it possible to determine an unknown specimen, but it also makes it possible for individuals, such as researchers in the field, workers in forensic professions or the general public, to conduct the measurements and determine an unknown individual. The expansion of this dataset will produce a more complete PCA plot that can be used as a reference database for the prediction of unknown extinct and extant specimens.

Limitations of GMM for Categorization

Categorization of phylogeny and function using geometric morphometry is seen within this study; however, there are limitations when it comes to GMM. All the specimens of this study need to be complete specimens. This limitation can make it difficult to find and add additional specimens into the dataset. It will be increasingly difficult with extinct specimens knowing that the majority of extinct fossils are found incomplete. Another limitation is the accessibility to collections. Digital collections are becoming more readily available but are still limited. The quality of 3D models plays a role when looking at shape variation. Models created using low-resolution data acquisition tools may not capture the detail of specific muscle attachments or an accurate representation of bone shape, which can have an effect on where the specimen plots within the PCA.

5. CONCLUSION:

The exploration of digital osteology collections with geometric morphometry led to the three main components of this study. The results from the landmark analysis show that a 50-sliding landmark method was an appropriate method when categorizing phylogeny and functionality in femur and humerus bones displaying the smallest amount of group overlap, total overlap among groups and a more accurate representation of shape variation. The PCA using the 50-sliding landmark method displayed results that were expected showing isolated groups at the lowest phylogenetic level. Taxonomic groups such as class, order, families and locomotor habits showed distinct groupings within the morphospace of the PCA consistent with preexisting knowledge that both phylogeny and functionality have an effect on bone shape. Categorization of phylogeny and functionality of all the specimens of this study through a PCA creates a reference database for identification of unknown specimens. The PC scores were converted to meristic ratios and additional specimens from outside the original dataset were measured and plotted within the morphospace of the PCA using the meristic ratios. The additional specimens all plotted within the appropriate locomotion groups as well as near specimens of similar class, order and family. The PCA produces results that are expected and categorize phylogeny and functionality, which then can be used by researchers in the field, workers in forensic professions or the general public to predict unknown specimens using simple meristic ratios. Input of models from additional osteology collections into this study will create an increased and more complete dataset that has the capability to be used as a reference database for identification of unknown specimens.

REFERENCES:

Adam, P.J., 2009, Hind Limb Anatomy: Encyclopedia of Marine Mammals, p. 562–565, doi: 10.1016/b978-0-12-373553-9.00130-9.

Adams, D.C., 2014, A Generalized K Statistic for Estimating Phylogenetic Signal from Shape and Other High-Dimensional Multivariate Data: Systematic Biology, v. 63, p. 685–697, doi: 10.1093/sysbio/syu030.

Adams, D.C., and Otárola-Castillo, E., 2013, Geomorph: an R package for the collection and analysis of geometric morphometric shape data: Methods in Ecology and Evolution, v. 4, p. 393–399, doi: 10.1111/2041-210x.12035.

Adams, D.C., Rohlf, F.J., and Slice, D.E., 2004, Geometric morphometrics: Ten years of progress following the 'revolution': Italian Journal of Zoology, v. 71, p. 5–16, doi: 10.1080/11250000409356545.

Adams, D.C., Rohlf, F.J., Slice, D.E., 2013, A field comes of age: geometric morphometrics in the 21st century: Hystrix, v. 24, p. 7–14, doi:10.4404/hystrix-24.1-6283

An, L., Fitzpatrick, D., and Harrison, P.M., 2016, Emergence and evolution of yeast prion and prion-like proteins: BMC Evolutionary Biology, v. 16, doi: 10.1186/s12862-016-0594-3.

Biancardi, C.M., and Minetti, A.E., 2012, Biomechanical determinants of transverse and rotary gallop in cursorial mammals: Journal of Experimental Biology, v. 215, p. 4144–4156, doi: 10.1242/jeb.073031.

Bookstein, F., 1996, Landmark methods for forms without landmarks: localizing group differences in outline shape: Proceedings of the Workshop on Mathematical Methods in Biomedical Image Analysis, doi: 10.1109/mmbia.1996.534080.

Ciccarelli, F.D., Doerks, T., Mering, C.V., Creevey, C.J., Snel, B. and Bork, P., 2006, Toward automatic reconstruction of a highly resolved tree of life: Science, v. 311, p. 1283-1287, doi: 10.1126/science.1123061.

Cooke, S.C.A.B., and Terhune, C.E., 2014, Form, Function, and Geometric Morphometrics: The Anatomical Record, v. 298, p. 5–28, doi: 10.1002/ar.23065.

Dial, K.P., 2003, Evolution Of Avian Locomotion: Correlates Of Flight Style, Locomotor Modules, Nesting Biology, Body Size, Development, And The Origin Of Flapping Flight: The Auk, v. 120, p. 941, doi: 10.1642/0004-8038(2003)120[0941:eoalco]2.0.co;2.

Dumont, M.C.A.F., Wall, C.E., Botton-Divet, L., Goswami, A., Peigné, S., and Fabre, A.-C., 2015, Do functional demands associated with locomotor habitat, diet, and activity pattern drive skull shape evolution in musteloid carnivorans?: Biological Journal of the Linnean Society, v. 117, p. 858–878, doi: 10.1111/bij.12719.

Elton, S. and Cardini, A., 2008, Anthropology from the desk? The challenges of the emerging era of data sharing: Journal of Anthropological Sciences, v. 86, p. 209-212.

Fabre, A.-C., Cornette, R., Peigné, S., and Goswami, A., 2013, Influence of body mass on the shape of forelimb in musteloid carnivorans: Biological Journal of the Linnean Society, v. 110, p. 91–103, doi: 10.1111/bij.12103.

Fabre, A.-C., Cornette, R., Goswami, A., and Peigné, S., 2015, Do constraints associated with the locomotor habitat drive the evolution of forelimb shape? A case study in musteloid carnivorans: Journal of Anatomy, v. 226, p. 596–610, doi: 10.1111/joa.12315.

Fu, X., Song, X., Li, X., Wong, K.K., Li, J., Zhang, F., Wang, C., and Wang, Z., 2017, Phylogenetic Tree Analysis of the Cold-Hot Nature of Traditional Chinese Marine Medicine for Possible Anticancer Activity: Evidence-Based Complementary and Alternative Medicine, v. 2017, p. 1–10, doi: 10.1155/2017/4365715.

Galland, M., and Friess, M., 2016, A three-dimensional geometric morphometrics view of the cranial shape variation and population history in the New World: American Journal of Human Biology, v. 28, p. 646–661, doi: 10.1002/ajhb.22845.

Gilbert, B.M., Martin, L.D., and Savage, H.G., 1985, Avian osteology: Flagstaff, AZ, Bone Books, 252 p.

Gippoliti, S., Amori, G., Castiglia, R., Colangelo, P., and Capanna, E., 2014, The relevance of Italian museum collections for research and conservation: the case of mammals: Rendiconti Lincei, v. 25, p. 351–357, doi: 10.1007/s12210-014-0304-2.

Gonzalez, P.N., Barbeito-Andrés, J., Daddona, L.A., Bernal, V., and Perez, S.I., 2016, Technical note: Performance of semi and fully automated approaches for registration of 3D surface coordinates in geometric morphometric studies: American Journal of Physical Anthropology, v. 160, p. 169–178, doi: 10.1002/ajpa.22934.

Gunz, P., Mitteroecker, P., and Bookstein, F.L., 2005, Semilandmarks in Three Dimensions: Developments in Primatology: Progress and Prospects Modern Morphometrics in Physical Anthropology, p. 73–98, doi: 10.1007/0-387-27614-9_3.

Hildebrand, M., 1974, Analysis of vertebrate structure: New York, John Wiley & Sons Inc, 728 p.

Hildebrand, M., and Goslow, G.E., 2001, Analysis of vertebrate structure: New York, John Wiley & Sons Inc, 660 p.

Holliday, T.W., and Friedl, L., 2013, Hominoid humeral morphology: 3D morphometric analysis: American Journal of Physical Anthropology, v. 152, p. 506–515, doi: 10.1002/ajpa.22385.

King, A.S., and MacLelland, J., 1985, Form and function in birds: London, Academic Press, v. 3, 522 p.

Kuzminsky, S.C., and Gardiner, M.S., 2012, Three-dimensional laser scanning: potential uses for museum conservation and scientific research: Journal of Archaeological Science, v. 39, p. 2744–2751, doi: 10.1016/j.jas.2012.04.020.

Leach, W.J., 1961, Functional anatomy: mammalian and comparative: New York, McGraw-Hill, 338 p.

Letunic, I., and Bork, P., 2006, Interactive Tree Of Life (iTOL): an online tool for phylogenetic tree display and annotation: Bioinformatics, v. 23, p. 127–128, doi: 10.1093/bioinformatics/btl529.

Letunic, I., and Bork, P., 2011, Interactive Tree Of Life v2: online annotation and display of phylogenetic trees made easy: Nucleic Acids Research, v. 39, doi: 10.1093/nar/gkr201.

Letunic, I., and Bork, P., 2016, Interactive tree of life (iTOL) v3: an online tool for the display and annotation of phylogenetic and other trees: Nucleic Acids Research, v. 44, doi: 10.1093/nar/gkw290.

Loy, A., 2007, Morphometrics and theriology homage to Marco Corti: Hystrix, the Italian Journal of Mammology, v. 18, p. 115-136.

Loy, A. and Slice, D.E., 2010, Image data banks and geometric morphometrics, *in* Luigi, P.N., and Vignes R.L., eds., Tools for Identifying Biodiversity: Progress and Problems, p. 243-248.

Maschner, H.D.G., Betts, M.W. and Schou, C.D., 2011, Virtual zooarchaeology of the Arctic project (VZAP): Virtual zooarchaeology of the Arctic project (VZAP): The SAA Archaeological Record, p. 41–43.

McGowan, C., and Mulock, J., 1999, A practical guide to vertebrate mechanics: Cambridge, Cambridge University Press, 316 p.

Miller, M. E., Christensen, G.C. and Evan, H.E., 1964, Anatomy of the dog: W. B. Saunders Company, 941 p.

Mitteroecker, P., and Gunz, P., 2009, Advances in Geometric Morphometrics: Evolutionary Biology, v. 36, p. 235–247, doi: 10.1007/s11692-009-9055-x.

Polly, P.D., 2007, Limbs in Mammalian Evolution, *in* Hall, B.K., ed., Fins into Limbs: Evolution, Development and Transformation, University of Chicago Press, p. 245–269.

R Development Core Team, 2012, R: A Language and Environment for Statistical Computing: http://cran.R-project.org (accessed January 2016).

Rohlf, F.J., 2000, Statistical power comparisons among alternative morphometric methods: American Journal of Physical Anthropology, v. 111, p. 463–478, doi: 10.1002/(sici)1096-8644(200004)111:4<463::aid-ajpa3>3.0.co;2-b.

Rohlf F.J., Marcus L.F., 1993, A revolution in morphometrics: Trends Ecology Evolution, v. 8, p. 129– 132.

Samuels, J.X., and Valkenburgh, B.V., 2008, Skeletal indicators of locomotor adaptations in living and extinct rodents: Journal of Morphology, v. 269, p. 1387–1411, doi: 10.1002/jmor.10662.

Samuels, J.X., Meachen, J.A., and Sakai, S.A., 2012, Postcranial morphology and the locomotor habits of living and extinct carnivorans: Journal of Morphology, v. 274, p. 121–146, doi: 10.1002/jmor.20077.

Savile, O.B.O., 1957, Adaptive evolution in the avian wing: Evolution, v. 11, p. 212–224, doi: 10.1111/j.1558-5646.1957.tb02889.x.

Slice D.E., 2007, Geometric morphometrics: Annual Review of Anthropology, v. 36 p. 261–281, doi: 10.1146/annurev.anthro.34.081804.120613

Appendix I: Individuals of study

Common Name	Class	Order	Family	Genus	Species
American Eider	Aves	Anseriformes	Anatidae	*Somateria*	*mollissima*
Arctic Fox	Mammalia	Carnivora	Canidae	*Vulpes*	*lagopus*
Arctic Loon	Aves	Gaviiformes	Gaviidae	*Gavia*	*arctica*
Arctic Tern	Aves	Charadriiformes	Sternidae	*Sterna*	*paradisaea*
Bald Eagle	Aves	Falconiformes	Accipitridae	*Haliaeetus*	*leucocephalus*
Bearded Seal	Mammalia	Carnivora	Phocidae	*Erignathus*	*barbatus*
Beaver	Mammalia	Rodentia	Castoridae	*Castor*	*canadensis*
Bison	Mammalia	Artiodactyla	Bovidae	*Bison*	*bison*
Black Bear	Mammalia	Carnivora	Ursidae	*Ursus*	*americanus*
Black Duck	Aves	Anseriformes	Anatidae	*Anas*	*rubripes*
Black Footed Albatross	Aves	Procellariiformes	Diomedeidae	*Phoebastria*	*nigripes*
Black Legged Kittiwake	Aves	Charadriiformes	Laridae	*Rissa*	*tridactyla*
Blue Winged Teal	Aves	Anseriformes	Anatidae	*Anas*	*discors*
Bobcat	Mammalia	Carnivora	Felidae	*Lynx*	*rufus*
Brant Goose	Aves	Anseriformes	Anatidae	*Branta*	*bernicla*
Canada Goose	Aves	Anseriformes	Anatidae	*Branta*	*canadensis*
Canada Lynx	Mammalia	Carnivora	Felidae	*Lynx*	*canadensis*
Canvasback	Aves	Anseriformes	Anatidae	*Aythya*	*valisineria*
Caribou	Mammalia	Artiodactyla	Cervidae	*Rangifer*	*tarandus*
Cassin's Auklet	Aves	Charadriiformes	Alcidae	*Ptychoramphus*	*aleuticus*
Common Goldeneye	Aves	Anseriformes	Anatidae	*Bucephala*	*clangula*
Common Loon	Aves	Gaviiformes	Gaviidae	*Gavia*	*immer*
Common Murre	Aves	Charadriiformes	Alcidae	*Uria*	*aalge*
Common Scoter	Aves	Anseriformes	Anatidae	*Melanitta*	*nigra*
Common Teal	Aves	Anseriformes	Anatidae	*Anas*	*crecca*
Common Tern	Aves	Charadriiformes	Sternidae	*Sterna*	*hirundo*

Common Name	Class	Order	Family	Genus	Species
Coyote	Mammalia	Carnivora	Canidae	*Canis*	*latrans*
Dall Sheep	Mammalia	Artiodactyla	Bovidae	*Ovis*	*dalli*
Fur Seal	Mammalia	Carnivora	Otariidae	*Callorhinus*	*ursinus*
Glaucous Gull	Aves	Charadriiformes	Laridae	*Larus*	*hyperboreus*
Gray Wolf	Mammalia	Carnivora	Canidae	*Canis*	*lupus*
Great Auk	Aves	Charadriiformes	Alcidae	*Pinguinus*	*impennis*
Great Horned Owl	Aves	Strigiformes	Strigidae	*Bubo*	*virginianus*
Greater Scaup	Aves	Anseriformes	Anatidae	*Aythya*	*marila*
Grey Seal	Mammalia	Carnivora	Phocidae	*Halichoerus*	*grypus*
Grizzly Bear	Mammalia	Carnivora	Ursidae	*Ursus*	*arctos*
Harbor Seal	Mammalia	Carnivora	Phocidae	*Phoca*	*vitulina*
Herring Gull	Aves	Charadriiformes	Laridae	*Larus*	*smithsonianus*
Hooded Seal	Mammalia	Carnivora	Phocidae	*Cystophora*	*cristata*
Horned Grebe	Aves	Podicipediformes	Podicipedidae	*Podiceps*	*auritus*
King Eider	Aves	Anseriformes	Anatidae	*Somateria*	*spectibilis*
Lesser Scaup	Aves	Anseriformes	Anatidae	*Aythya*	*affinis*
Little Auk	Ave	Charadriiformes	Alcidae	*Alle*	*alle*
Long Tailed Duck	Aves	Anseriformes	Anatidae	*Clangula*	*hyemalis*
Male Mule Deer	Mammalia	Artiodactyla	Cervidae	*Odocoileus*	*hemionus*
Mallard	Aves	Anseriformes	Anatidae	*Anas*	*platyrhynchos*
Mink	Mammalia	Carnivora	Mustelidae	*Neovison*	*vison*
Moose	Mammalia	Artiodactyla	Cervidae	*Alces*	*alces*
Musk Ox	Mammalia	Artiodactyla	Bovidae	*Ovibos*	*moschatus*
Northern Gannet	Aves	Suliformes	Sulidae	*Morus*	*bassanus*
Northern Pintail	Aves	Anseriformes	Anatidae	*Anas*	*acuta*
Northern Raven	Aves	Passeriformes	Corvidae	*Corvus*	*corax*
Northern Shoveler	Aves	Anseriformes	Anatidae	*Anas*	*clypeata*
Osprey	Aves	Accipitriformes	Pandionidae	*Pandion*	*haliaetus*

Common Name	Class	Order	Family	Genus	Species
Pacific Loon	Aves	Gaviiformes	Gaviidae	*Gavia*	*pacifica*
Parasitic Skua	Aves	Charadriiformes	Stercorariidae	*Stercorarius*	*parasiticus*
Pigeon Guillemot	Aves	Charadriiformes	Alcidae	*Cepphus*	*columba*
Polar Bear	Mammalia	Carnivora	Ursidae	*Ursus*	*maritimus*
Pomarine Skua	Aves	Charadriiformes	Stercorariidae	*Stercorarius*	*pomarinus*
Porcupine	Mammalia	Rodentia	Erethizontidae	*Erethizon*	*dorsatum*
Red Breasted Merganser	Aves	Anseriformes	Anatidae	*Mergus*	*serrator*
Red Fox	Mammalia	Carnivora	Canidae	*Vulpes*	*vulpes*
Red Necked Grebe	Aves	Podicipediformes	Podicipedidae	*Podiceps*	*grisegena*
Red Tailed Hawk	Aves	Accipitriformes	Accipitridae	*Buteo*	*jamaicensis*
Red Throated Loon	Aves	Gaviiformes	Gaviidae	*Gavia*	*stellata*
Ringed Seal	Mammalia	Carnivora	Phocidae	*Pusa*	*hispida*
Rock Ptarmigan	Aves	Galliformes	Phasianidae	*Lagopus*	*muta*
Rough Legged Hawk	Aves	Falconiformes	Accipitridae	*Buteo*	*lagopus*
Sage Grouse	Aves	Galliformes	Tetraonidae	*Centrocercus*	*urophasianus*
Sea Lion	Mammalia	Carnivora	Otariidae	*Zalophus*	*californianus*
Sea Otter	Mammalia	Carnivora	Mustelidae	*Enhydra*	*lutris*
Sharp Tailed Grouse	Aves	Galliformes	Phasianidae	*Tympanuchus*	*phasianellus*
Snowy Owl	Aves	Strigiformes	Strigidae	*Bubo*	*scandiacus*
Spruce Grouse	Aves	Galliformes	Phasianidae	*Falcipennis*	*canadensis*
Squirrel	Mammalia	Rodentia	Sciuridae	*Sciurus*	*carolinensis*
Thick Billed Murre	Aves	Charadriiformes	Alcidae	*Uria*	*lomvia*
Trumpeter Swan	Aves	Anseriformes	Anatidae	*Cygnus*	*buccinator*
Tufted puffin	Aves	Charadriiformes	Alcidae	*Fratercula*	*cirrhata*
Tundra Swan	Aves	Anseriformes	Anatidae	*Cygnus*	*columbianus*
Walrus	Mammalia	Carnivora	Odobenidae	*Odobenus*	*rosmarus*
White Fronted Goose	Aves	Anseriformes	Anatidae	*Anser*	*albifrons*

Common Name	Class	Order	Family	Genus	Species
Willow Ptarmigan	Aves	Galliformes	Phasianidae	*Lagopus*	*lagopus*
Wolverine	Mammalia	Carnivora	Mustelidae	*Gulo*	*gulo*
Wood Duck	Aves	Anseriformes	Anatidae	*Aix*	*sponsa*

Appendix II: Femora individuals of study

Common Name	Class	Order	Family	Genus	Species
American Eider	Aves	Anseriformes	Anatidae	*Somateria*	*mollissima*
Arctic Fox	Mammalia	Carnivora	Canidae	*Vulpes*	*lagopus*
Bald Eagle	Aves	Falconiformes	Accipitridae	*Haliaeetus*	*leucocephalus*
Bearded Seal	Mammalia	Carnivora	Phocidae	*Erignathus*	*barbatus*
Beaver	Mammalia	Rodentia	Castoridae	*Castor*	*canadensis*
Bison	Mammalia	Artiodactyla	Bovidae	*Bison*	*bison*
Black Bear	Mammalia	Carnivora	Ursidae	*Ursus*	*americanus*
Black Duck	Aves	Anseriformes	Anatidae	*Anas*	*rubripes*
Black Legged Kittiwake	Aves	Charadriiformes	Laridae	*Rissa*	*tridactyla*
Blue Winged Teal	Aves	Anseriformes	Anatidae	*Anas*	*discors*
Bobcat	Mammalia	Carnivora	Felidae	*Lynx*	*rufus*
Canada Goose	Aves	Anseriformes	Anatidae	*Branta*	*canadensis*
Canada Lynx	Mammalia	Carnivora	Felidae	*Lynx*	*canadensis*
Canvasback	Aves	Anseriformes	Anatidae	*Aythya*	*valisineria*
Caribou	Mammalia	Artiodactyla	Cervidae	*Rangifer*	*tarandus*
Cassin's Auklet	Aves	Charadriiformes	Alcidae	*Ptychoramphus*	*aleuticus*
Common Goldeneye	Aves	Anseriformes	Anatidae	*Bucephala*	*clangula*
Common Loon	Aves	Gaviiformes	Gaviidae	*Gavia*	*immer*
Common Scoter	Aves	Anseriformes	Anatidae	*Melanitta*	*nigra*
Common Teal	Aves	Anseriformes	Anatidae	*Anas*	*crecca*
Common Tern	Aves	Charadriiformes	Sternidae	*Sterna*	*hirundo*
Coyote	Mammalia	Carnivora	Canidae	*Canis*	*latrans*
Dall Sheep	Mammalia	Artiodactyla	Bovidae	*Ovis*	*dalli*
Great Horned Owl	Aves	Strigiformes	Strigidae	*Bubo*	*virginianus*
Greater Scaup	Aves	Anseriformes	Anatidae	*Aythya*	*marila*
Grey Seal	Mammalia	Carnivora	Phocidae	*Halichoerus*	*grypus*

Common Name	Class	Order	Family	Genus	Species
Grizzly Bear	Mammalia	Carnivora	Ursidae	*Ursus*	*arctos*
Harbor Seal	Mammalia	Carnivora	Phocidae	*Phoca*	*vitulina*
Herring Gull	Aves	Charadriiformes	Laridae	*Larus*	*smithsonianus*
Hooded Seal	Mammalia	Carnivora	Phocidae	*Cystophora*	*cristata*
King Eider	Aves	Anseriformes	Anatidae	*Somateria*	*spectibilis*
Lesser Scaup	Aves	Anseriformes	Anatidae	*Aythya*	*affinis*
Little Auk	Ave	Charadriiformes	Alcidae	*Alle*	*alle*
Long Tailed Duck	Aves	Anseriformes	Anatidae	*Clangula*	*hyemalis*
Male Mule Deer	Mammalia	Artiodactyla	Cervidae	*Odocoileus*	*hemionus*
Mallard	Aves	Anseriformes	Anatidae	*Anas*	*platyrhynchos*
Mink	Mammalia	Carnivora	Mustelidae	*Neovison*	*vison*
Moose	Mammalia	Artiodactyla	Cervidae	*Alces*	*alces*
Musk Ox	Mammalia	Artiodactyla	Bovidae	*Ovibos*	*moschatus*
Northern Gannet	Aves	Suliformes	Sulidae	*Morus*	*bassanus*
Northern Pintail	Aves	Anseriformes	Anatidae	*Anas*	*acuta*
Northern Raven	Aves	Passeriformes	Corvidae	*Corvus*	*corax*
Osprey	Aves	Accipitriformes	Pandionidae	*Pandion*	*haliaetus*
Pacific Loon	Aves	Gaviiformes	Gaviidae	*Gavia*	*pacifica*
Parasitic Skua	Aves	Charadriiformes	Stercorariidae	*Stercorarius*	*parasiticus*
Pigeon Guillemot	Aves	Charadriiformes	Alcidae	*Cepphus*	*columba*
Polar Bear	Mammalia	Carnivora	Ursidae	*Ursus*	*maritimus*
Pomarine Skua	Aves	Charadriiformes	Stercorariidae	*Stercorarius*	*pomarinus*
Porcupine	Mammalia	Rodentia	Erethizontidae	*Erethizon*	*dorsatum*
Red Breasted Merganser	Aves	Anseriformes	Anatidae	*Mergus*	*serrator*
Red Fox	Mammalia	Carnivora	Canidae	*Vulpes*	*vulpes*
Red Necked Grebe	Aves	Podicipediformes	Podicipedidae	*Podiceps*	*grisegena*
Red Tailed Hawk	Aves	Accipitriformes	Accipitridae	*Buteo*	*jamaicensis*

Common Name	**Class**	**Order**	**Family**	**Genus**	**Species**
Red Throated Loon	Aves	Gaviiformes	Gaviidae	*Gavia*	*stellata*
Ringed Seal	Mammalia	Carnivora	Phocidae	*Pusa*	*hispida*
Rock Ptarmigan	Aves	Galliformes	Phasianidae	*Lagopus*	*muta*
Rough Legged Hawk	Aves	Falconiformes	Accipitridae	*Buteo*	*lagopus*
Sea Otter	Mammalia	Carnivora	Mustelidae	*Enhydra*	*lutris*
Sharp Tailed Grouse	Aves	Galliformes	Phasianidae	*Tympanuchus*	*phasianellus*
Snowy Owl	Aves	Strigiformes	Strigidae	*Bubo*	*scandiacus*
Spruce Grouse	Aves	Galliformes	Phasianidae	*Falcipennis*	*canadensis*
Squirrel	Mammalia	Rodentia	Sciuridae	*Sciurus*	*carolinensis*
Thick Billed Murre	Aves	Charadriiformes	Alcidae	*Uria*	*lomvia*
Trumpeter Swan	Aves	Anseriformes	Anatidae	*Cygnus*	*buccinator*
Tundra Swan	Aves	Anseriformes	Anatidae	*Cygnus*	*columbianus*
Walrus	Mammalia	Carnivora	Odobenidae	*Odobenus*	*rosmarus*
White Fronted Goose	Aves	Anseriformes	Anatidae	*Anser*	*albifrons*
Wolverine	Mammalia	Carnivora	Mustelidae	*Gulo*	*gulo*
Wood Duck	Aves	Anseriformes	Anatidae	*Aix*	*sponsa*

Appendix III: Humeri individuals of study

Common Name	Class	Order	Family	Genus	Species
American Eider	Aves	Anseriformes	Anatidae	*Somateria*	*mollissima*
Arctic Loon	Aves	Gaviiformes	Gaviidae	*Gavia*	*arctica*
Arctic Tern	Aves	Charadriiformes	Sternidae	*Sterna*	*paradisaea*
Bald Eagle	Aves	Falconiformes	Accipitridae	*Haliaeetus*	*leucocephalus*
Bearded Seal	Mammalia	Carnivora	Phocidae	*Erignathus*	*barbatus*
Beaver	Mammalia	Rodentia	Castoridae	*Castor*	*canadensis*
Bison	Mammalia	Artiodactyla	Bovidae	*Bison*	*bison*
Black Legged Kittiwake	Aves	Charadriiformes	Laridae	*Rissa*	*tridactyla*
Blue Winged Teal	Aves	Anseriformes	Anatidae	*Anas*	*discors*
Canada Goose	Aves	Anseriformes	Anatidae	*Branta*	*canadensis*
Canada Lynx	Mammalia	Carnivora	Felidae	*Lynx*	*canadensis*
Cassin's Auklet	Aves	Charadriiformes	Alcidae	*Ptychoramphus*	*aleuticus*
Common Goldeneye	Aves	Anseriformes	Anatidae	*Bucephala*	*clangula*
Common Loon	Aves	Gaviiformes	Gaviidae	*Gavia*	*immer*
Common Murre	Aves	Charadriiformes	Alcidae	*Uria*	*aalge*
Common Scoter	Aves	Anseriformes	Anatidae	*Melanitta*	*nigra*
Common Teal	Aves	Anseriformes	Anatidae	*Anas*	*crecca*
Common Tern	Aves	Charadriiformes	Sternidae	*Sterna*	*hirundo*
Coyote	Mammalia	Carnivora	Canidae	*Canis*	*latrans*
Fur Seal	Mammalia	Carnivora	Otariidae	*Callorhinus*	*ursinus*
Glaucous Gull	Aves	Charadriiformes	Laridae	*Larus*	*hyperboreus*
Gray Wolf	Mammalia	Carnivora	Canidae	*Canis*	*lupus*
Great Auk	Aves	Charadriiformes	Alcidae	*Pinguinus*	*impennis*
Great Horned Owl	Aves	Strigiformes	Strigidae	*Bubo*	*virginianus*
Greater Scaup	Aves	Anseriformes	Anatidae	*Aythya*	*marila*
Grey Seal	Mammalia	Carnivora	Phocidae	*Halichoerus*	*grypus*

Common Name	**Class**	**Order**	**Family**	**Genus**	**Species**
Grizzly Bear	Mammalia	Carnivora	Ursidae	*Ursus*	*arctos*
Herring Gull	Aves	Charadriiformes	Laridae	*Larus*	*smithsonianus*
Hooded Seal	Mammalia	Carnivora	Phocidae	*Cystophora*	*cristata*
Horned Grebe	Aves	Podicipediformes	Podicipedidae	*Podiceps*	*auritus*
Lesser Scaup	Aves	Anseriformes	Anatidae	*Aythya*	*affinis*
Little Auk	Ave	Charadriiformes	Alcidae	*Alle*	*alle*
Mallard	Aves	Anseriformes	Anatidae	*Anas*	*platyrhynchos*
Mink	Mammalia	Carnivora	Mustelidae	*Neovison*	*vison*
Musk Ox	Mammalia	Artiodactyla	Bovidae	*Ovibos*	*moschatus*
Northern Gannet	Aves	Suliformes	Sulidae	*Morus*	*bassanus*
Northern Pintail	Aves	Anseriformes	Anatidae	*Anas*	*acuta*
Northern Raven	Aves	Passeriformes	Corvidae	*Corvus*	*corax*
Northern Shoveler	Aves	Anseriformes	Anatidae	*Anas*	*clypeata*
Pacific Loon	Aves	Gaviiformes	Gaviidae	*Gavia*	*pacifica*
Parasitic Skua	Aves	Charadriiformes	Stercorariidae	*Stercorarius*	*parasiticus*
Pigeon Guillemot	Aves	Charadriiformes	Alcidae	*Cepphus*	*columba*
Polar Bear	Mammalia	Carnivora	Ursidae	*Ursus*	*maritimus*
Pomarine Skua	Aves	Charadriiformes	Stercorariidae	*Stercorarius*	*pomarinus*
Porcupine	Mammalia	Rodentia	Erethizontidae	*Erethizon*	*dorsatum*
Red Breasted Merganser	Aves	Anseriformes	Anatidae	*Mergus*	*serrator*
Red Necked Grebe	Aves	Podicipediformes	Podicipedidae	*Podiceps*	*grisegena*
Red Tailed Hawk	Aves	Accipitriformes	Accipitridae	*Buteo*	*jamaicensis*
Ringed Seal	Mammalia	Carnivora	Phocidae	*Pusa*	*hispida*
Rock Ptarmigan	Aves	Galliformes	Phasianidae	*Lagopus*	*muta*
Sage Grouse	Aves	Galliformes	Tetraonidae	*Centrocercus*	*urophasianus*
Sea Lion	Mammalia	Carnivora	Otariidae	*Zalophus*	*californianus*
Sea Otter	Mammalia	Carnivora	Mustelidae	*Enhydra*	*lutris*

Common Name	**Class**	**Order**	**Family**	**Genus**	**Species**
Sharp Tailed Grouse	Aves	Galliformes	Phasianidae	*Tympanuchus*	*phasianellus*
Snowy Owl	Aves	Strigiformes	Strigidae	*Bubo*	*scandiacus*
Spruce Grouse	Aves	Galliformes	Phasianidae	*Falcipennis*	*canadensis*
Squirrel	Mammalia	Rodentia	Sciuridae	*Sciurus*	*carolinensis*
Thick Billed Murre	Aves	Charadriiformes	Alcidae	*Uria*	*lomvia*
Walrus	Mammalia	Carnivora	Odobenidae	*Odobenus*	*rosmarus*
White Fronted Goose	Aves	Anseriformes	Anatidae	*Anser*	*albifrons*
Wolverine	Mammalia	Carnivora	Mustelidae	*Gulo*	*gulo*
Wood Duck	Aves	Anseriformes	Anatidae	*Aix*	*sponsa*

Appendix IV: Meristic ratios of femora

Common Name	H/W Ratio	W/D Ratio
Ringed Seal	1.66	2.12
Hooded Seal	1.74	1.96
Grey Seal	1.79	1.71
Bearded Seal	1.81	1.69
Harbor Seal	2.01	2.02
Walrus	2.07	2.18
Sea Otter	2.54	1.07
Beaver	2.58	1.35
Red Throated Loon	2.73	3.31
Bison	2.75	0.81
Pacific Loon	2.88	2.59
Common Loon	3.3	2.64
Red Necked Grebe	3.3	1.88
Musk Ox	3.32	0.8
Porcupine	3.56	1.22
Moose	3.71	0.81
Mink	3.94	0.91
Wolverine	3.94	1.01
Black Bear	3.95	1.1
Grizzly Bear	4.06	1.13
Trumpeter Swan	4.1	1.62
Tundra Swan	4.15	1.45
Polar Bear	4.2	1.09
Male Mule Deer	4.25	0.78
Red Breasted Merganser	4.26	1.48
American Eider	4.28	1.64
Caribou	4.28	0.77
Dall Sheep	4.31	0.84
Bald Eagle	4.34	1.14
Squirrel	4.37	1.07
Lesser Scaup	4.41	1.25
King Eider	4.42	1.46
Canvasback	4.45	1.19
Common Scoter (Black)	4.51	1.38
Greater Scaup	4.51	1.34
White Fronted Goose	4.53	1.36
Snowy Owl	4.65	1.57
Osprey	4.66	1.11

Common Name	H/W Ratio	W/D Ratio
Canada Goose	4.69	1.42
Blue Winged Teal	4.73	1.46
Long Tailed Duck	4.73	1.61
Common Goldeneye	4.75	1.41
Wood Duck	4.75	1.13
Mallard	4.83	1.33
Northern Gannet	4.83	1.41
Black Duck	4.91	1.44
Arctic Fox	5	0.92
Northern Raven	5.03	1.63
Northern Pintail	5.07	1.41
Common Teal	5.08	1.65
Bobcat	5.19	1.1
Black Legged Kittiwake	5.21	1.53
Red Tailed Hawk	5.26	1.26
Herring Gull	5.29	1.65
Thick Billed Murre	5.31	1.41
Pomarine Skua	5.34	1.41
Sharp Tailed Grouse	5.34	1.14
Rough Legged Hawk	5.35	1.21
Coyote	5.39	0.91
Rock Ptarmigan	5.44	1.19
Cassin's Auklet	5.48	1.37
Red Fox	5.55	0.83
Great Horned Owl	5.62	1.55
Parasitic Skua	5.62	1.43
Pigeon Guillemot	5.69	1.45
Little Auk	5.83	1.4
Canada Lynx	6.15	1.01
Common Tern	6.33	1.57
Spruce Grouse	6.4	1.24
Sabertooth Cat (Smilodon)	4.45	1.07
Bison *latifrons*	3.46	0.83
Sloth	2.61	1.48
Hagerman Horse	4.05	0.78
Big Horn Sheep	4.8	0.86
Bison	3.88	0.82
Brown Pelican	3.87	1.35
Elk	4.01	0.81

Common Name	H/W Ratio	W/D Ratio
Emperor Penguin	4.09	1.18
Fisher	5.53	1.02
Giraffe	4.06	0.7
Leopard	5.22	1.02
Mountain Goat	4.99	0.82
Pronghorn	5.09	0.78
Ringed Seal	1.51	2.04
Sandhill Crane	4.6	1.14
Sea Otter	3.16	1.07
Walrus	1.63	2.1

Appendix V: Meristic ratios of humeri

Common Name	H/W	D/W
American Eider	6.72	0.69
Arctic Loon	6.76	0.68
Arctic Tern	6.69	0.71
Bald Eagle	5.92	0.66
Bearded Seal	2.6	2.36
Beaver	2.57	1.64
Big Horn Sheep	4.8	2.71
Bison	3.53	2.68
Bison	3.99	2.66
Bison *latifrons*	3.19	2.6
Black Legged Kittiwake	5.98	0.56
Blue Winged Teal	6.26	0.93
Brown Pelican	7.54	0.64
Canada Goose	6.93	0.7
Canada Lynx	5.5	1.96
Cassin's Auklet	7.1	0.75
Common Goldeneye	6.59	0.9
Common Loon	10.89	0.81
Common Murre	8.73	0.92
Common Scoter	7.48	0.95
Common Teal	6.28	0.99
Common Tern	7.16	0.73
Coyote	5.83	2.1
Emperor Penguin	3.4	0.79
Fisher	4.36	1.62
Fur Seal	2.6	1.96
Giraffe	3.76	1.7
Glaucous Gull	7.12	0.77
Gray Wolf	4.66	1.94
Great Auk	7.31	0.88
Great Horned Owl	6.18	0.73
Greater Scaup	7.62	0.91
Grey Seal	2.76	2.14
Grizzly Bear	3.12	2.26
Hagerman Horse	3.59	2.97
Herring Gull	7.75	0.83
Hooded Seal	2.78	2.01
Horned Grebe	10.27	0.76

Common Name	H/W	D/W
Leopard	4.04	1.72
Lesser Scaup	6.92	1.12
Little Auk	6.96	0.81
Mallard	6.1	0.89
Mink	3.88	2.17
Mountain Goat	5.04	2.05
Musk Ox	4.15	2.6
Northern Gannet	10.42	0.53
Northern Pintail	6.42	0.95
Northern Raven	4.73	0.72
Northern Shoveler	6.85	0.96
Pacific Loon	8.56	0.92
Parasitic Skua	7.27	0.89
Pigeon Guillemot	7.77	0.76
Polar Bear	3.22	2.32
Pomarine Skua	7.32	0.83
Porcupine	3.84	1.6
Pronghorn	5.02	2.18
Red Breasted Merganser	7.06	0.8
Red Necked Grebe	9.63	0.73
Red Tailed Hawk	5.83	0.81
Ringed Seal	2.46	1.81
Ringed Seal	2.55	2.08
Rock Ptarmigan	5.23	0.85
Saber-toothed Cat (Smilodon)	3.56	1.8
Sage Grouse	5.04	0.81
Sandhill Crane	6.49	0.72
Sea Otter	2.96	2
SeaLion2	2.25	2.18
Sharp Tailed Grouse	4.94	0.96
Snowy Owl	6.02	0.72
Spruce Grouse	5.31	0.94
Squirrel	3.74	1.79
Thick Billed Murre	7.53	0.9
Walrus	2.7	1.9
Walrus	2.62	1.87
White Fronted Goose	6.83	0.79
Wolverine	3.6	2.07
Wood Duck	6.2	0.76